frontiers in Earth Science

REVIEW
published: 13 June 2018
doi: 10.3389/feart.2018.00056

Understanding Fast and Slow Unrest at Volcanoes and Implications for Eruption Forecasting

*John Stix**

Department of Earth and Planetary Sciences, McGill University, Montreal, QC, Canada

This paper examines the behavior of volcanoes that erupt quickly with paroxysmal explosive eruptions, and other volcanoes that erupt over extended periods without such paroxysmal activity. "Fast" activity typically occurs over the course of months to years, including precursory unrest, the paroxysmal eruption itself, and post-paroxysmal activity. "Slow" activity comprises extended restlessness over the course of decades, and eruptions are typically small and sometimes uncommon. I review activity at eight volcanoes with fast and slow activity, highlighting the main events, and commonalities in behavior among the different systems. In terms of forecasting, volcanoes with fast unrest typically have short 1–3 month precursory periods prior to the climactic eruption, while volcanoes with slow unrest commonly have an extended period of considerable uncertainty regarding the presence or absence of new magma, as well as unanticipated accelerations in activity. Volcanoes with fast behavior are associated with magmas having elevated volatile contents (up to ∼7 wt. % H_2O), rapid magma ascent rates, and rapid declines in activity after the climactic eruption. These volcanoes also exhibit well-defined magma plumbing systems containing mobile volatile-rich magma, with the plumbing system often sealed between the top of the shallow magma reservoir and the surface prior to the climactic eruption. Volcanoes with slow behavior have complex plumbing systems comprising cracks, fractures, dykes, and sills and magmas that are crystal-rich, partly degassed, and rheologically sluggish. These volcanoes experience a progressive opening of their systems as magma intrudes and fractures country rock, allowing degassing to occur. The degree to which a system is opened is determined by the rate at which new magma is emplaced at shallow levels. As such, magma emplacement rates which are fast, intermediate, or slow should produce unrest on similar timescales. Slower rates of emplacement enhance the opening process due to a cumulatively high number of fractures and increased fracture density which develop during the extended period of unrest. Many systems both fast and slow receive inputs of more mafic magma which can drive activity seen at the surface. A series of recently developed tools is examined and discussed in order to provide an improved means of forecasting activity at both types of volcanoes. These include assessment of early phreatic activity and associated gases, V_p/V_s ratios of magma by seismic tomography, and estimates of magma volume from precursory seismicity. What is required now are protocols which integrate these approaches in a manner which is useful for accurate forecasting.

Keywords: fast unrest, slow unrest, eruption mechanisms, eruption dynamics, precursory activity

OPEN ACCESS

Edited by:
Shanaka L. de Silva,
Oregon State University, United States

Reviewed by:
Greg A. Valentine,
University at Buffalo, United States
Jan Marie Lindsay,
University of Auckland, New Zealand

***Correspondence:**
John Stix
stix@eps.mcgill.ca

Specialty section:
This article was submitted to Volcanology, a section of the journal Frontiers in Earth Science

Received: *26 January 2018*
Accepted: *03 May 2018*
Published: *13 June 2018*

Citation:
Stix J (2018) Understanding Fast and Slow Unrest at Volcanoes and Implications for Eruption Forecasting. Front. Earth Sci. 6:56. doi: 10.3389/feart.2018.00056

INTRODUCTION

Volcanoes exhibit a range of eruptive styles. One type of end-member behavior, as exemplified by volcanoes such as Hekla in Iceland and Cerro Negro in Nicaragua, awaken nearly instantaneously with essentially no warning. They reach their peak intensity very quickly within the space of hours, with subsequent activity decaying to background levels over the space of days, weeks, or months. The other end-member includes volcanoes which are continually in eruption, such as Santiaguito (Guatemala), Stromboli (Italy), and Yasur (Vanuatu). But these end-member styles constitute a very small number of volcanoes. More commonly, volcanoes of intermediate to silicic composition exhibit "fast" or "slow" behavior, although some systems show characteristics of both fast and slow activity. The differences can be observed both during the early and late stages of unrest. Volcanoes with fast activity exhibit a period of precursory unrest lasting several months prior to the principal eruption or eruptions (**Figure 1**), implying rapid magma emplacement and/or ascent. Likewise, these volcanoes return rapidly to a state of quiescence, commonly over timescales of weeks or months. By contrast, volcanoes exhibiting slow behavior escalate their activity over years to decades to their point of "peak" activity, implying slow, fitful rise of magma which may never reach the surface. Such volcanoes may not necessarily show a climactic phase; instead, periods of enhanced activity, such as higher rates of dome growth or explosive activity, are more common. These slow volcanic systems commonly require years to decades before they can be considered inactive.

The fast and slow behavior discussed in this paper is not always obvious and straightforward to classify. The current slow activity of Popocatépetl, now approaching 30 years in duration, has exhibited periods of rapidly accelerating activity including explosive eruptions, most notably in December 2000. By contrast, fast behavior at Mt. St. Helens in 1980 was followed by 6 years of comparatively low-level slow activity.

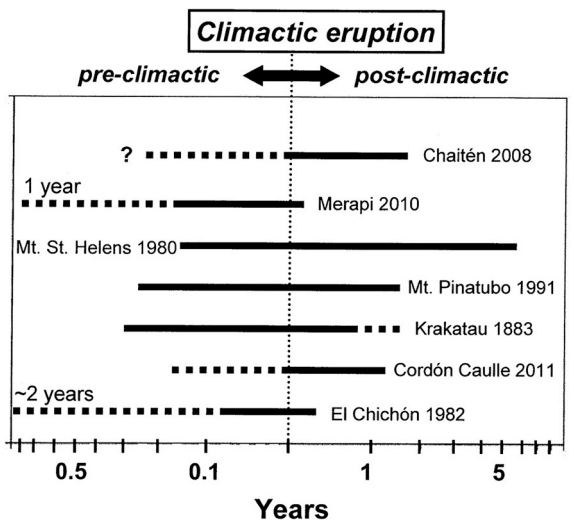

FIGURE 1 | Timescales of activity at fast volcanic systems, including precursory activity, climactic activity, and waning activity. Dashed lines indicate uncertainty in durations. For Chaitén, Pinatubo, and Krakatau, the degree of uncertainty is larger because these volcanoes were not monitored prior to the climactic eruptions.

A further caveat is that during their lifetimes, these types of volcanoes may exhibit fast behavior during certain periods of unrest and slow activity during other periods. There also may be unrest intervals where mixed activity occurs. For example, some unrest periods typically comprise several months or years of seismicity, degassing, and explosions. Here I am concerned with (a) unrest comprising paroxysmal eruptions, preceded, and followed by short periods of activity generally on the timescale of months (fast systems), and (b) unrest lasting more than a decade, with periods of strong degassing, seismic activity, and comparatively low-level explosive activity (slow systems).

Hence this paper explores the salient characteristics of fast and slow behavior. It is both a review which compares and contrasts eight well-documented volcanic systems and also a conceptual study which examines the physical processes involved and their geophysical and geochemical manifestations. The main purpose of the paper is to (1) illustrate the differences between volcanoes which re-activate quickly and those that re-activate slowly, and (2) propose an integrated means of forecasting such activity. I first examine four volcanoes with fast activity and four with slow activity, then show and discuss their common features. I then discuss the nature of the magma-hydrothermal system beneath these volcanoes and the concept of "closed" and "open" plumbing systems between the magma and the surface. Lastly I examine several new ways forward for forecasting eruptions at these types of volcanoes.

To illustrate fast behavior, I examine the 2008 eruption of Chaitén in Chile, the 2010 eruption of Merapi in Indonesia, the 1980 Mt. St. Helens eruption in the USA, and the 1991 Mount Pinatubo eruption in the Philippines. These examples are generally well-studied and illustrate fast behavior at a range of timescales. For examples of extended unrest (slow systems), I have chosen Soufrière Hills volcano on the island of Montserrat, Turrialba volcano in Costa Rica, Popocatépetl in Mexico, and Nevado del Ruiz in Colombia. These systems again have good datasets, they have been active for many years, and significantly, they remain restless as of this writing.

This paper is complementary to the recent study by Sparks and Cashman (2017), which also examines fast and slow behavior of magmatic systems for a different set of timescales. They attribute "slow" behavior of 10^3–10^5 years to melt-associated and mush-associated processes of magmas resident in reservoirs at various depths in the crust. On these slow timescales, the different reservoirs remain distinct. By contrast, "fast" behavior of 10^{-2}–10^2 years is characteristic for erupting magmas, driven by the different reservoirs becoming interconnected at various spatial and temporal scales.

FOUR VOLCANOES WITH FAST ACTIVITY

Chaitén, Chile, 2008–2009

Chaitén is a rhyolitic volcano which last erupted in the seventeenth century (Lara et al., 2013) prior to re-activating and

TABLE 1 | Characteristics of fast volcanic systems.

Volcano	Chaitén	Merapi	Mt. St. Helens	Mt. Pinatubo
Date of initial precursory activity	Unknown	31-Oct-2009	15-Mar-1980	15-Mar-1991
Date of climactic eruption(s)	2, 6, 8 May 2008	5-Nov-2010	18-May-1980	15-Jun-1991
VEI of climactic eruption(s) (data from https://volcano.si.edu)	4	4	5	6
Elapsed time between first activity and climactic eruption (months)	Unknown	12	2	3
Type of precursory activity	Earthquakes	Earthquakes, inflation	Earthquakes, inflation, phreatic+ phreatomagmatic eruptions	Earthquakes. SO_2 release, phreatic eruptions, dome emplacement, magmatic explosions
DRE volume of climactic magma erupted (km^3)	∼0.3	0.02–0.05	0.24	3.7–5.3
Composition of climactic magma	Rhyolite	Basaltic andesite	Dacite	Dacite
Maximum water content of climactic magma (wt. %)	4	6.6	6.7	6.4
Crystal content of climactic magma (vol. %)	0	30–60	∼40	15–47
End date of activity	Late 2009 or earliest 2010	End November 2010	Late October 1986	End October 1992
Elapsed time between climactic eruption and end of activity (months)	∼20	∼1	77	16.5
Evidence for mafic magma?	Yes	?	?	Yes
Sources of data	Castro and Dingwell, 2009	Budi-Santoso et al., 2013	Blundy et al., 2008	Daag et al., 1996
	Major and Lara, 2013	Drignon et al., 2016	Carey and Sigurdsson, 1985	Harlow et al., 1996
	Pallister et al., 2013	Surono et al., 2012	Cashman and Hoblitt, 2004	Pallister et al., 1996
			Christiansen and Peterson, 1981	Rutherford and Devine, 1996
			Endo et al., 1981	Sabit et al., 1996
			Lipman et al., 1981	Scott et al., 1996
			Moore and Albee, 1981	White, 1996
			Rutherford et al., 1985 Sarna-Wojcicki et al., 1981	Wolfe and Hoblitt, 1996

erupting for 20 months in 2008–2009. Tephra fall and pyroclastic density current deposits dated at ∼9.4 ka may be associated with the summit caldera of the volcano (Naranjo and Stern, 2004). During the 2008–2009 activity, a series of large rhyolitic explosive eruptions beginning 1 May 2008 lasted a little more than a week, with plinian columns of VEI 4 reaching ∼20 km observed on 2, 6, and 8 May (Major and Lara, 2013) (**Table 1**). After 8 May explosive activity declined appreciably, with simultaneous explosive and effusive eruption of rhyolitic magma until the end of May. Thereafter, a series of lava domes were emplaced to late 2009 or earliest 2010 when the eruption stopped (Pallister et al., 2013). The bulk of lava extrusion occurred from May to September 2008. A total of 1.1 km^3 DRE of rhyolitic magma was erupted, 0.3 km^3 explosively and 0.8 km^3 effusively (Major and Lara, 2013).

The rhyolite erupted from Chaitén has several interesting characteristics. It is crystal-poor, and petrology indicates elevated temperatures of ∼800°C compared to typical rhyolites (600–700°C), as well as high volatile contents of up to 4 wt. % H_2O (Castro and Dingwell, 2009) (**Table 1**). The magma may have contained even higher water contents if stored at 5–10 km or deeper (Wicks et al., 2011), and it also may have been bubbly prior to eruption. As discussed by Castro and Dingwell (2009), these characteristics are the hallmark of low-viscosity rhyolitic magma, allowing its rapid rise during both the initial explosive phase and later effusive phase.

A key question at Chaitén is the timing of precursory activity. Published accounts state that felt earthquakes in the town of Chaitén began on 30 April, just 1 day before the eruption started (Castro and Dingwell, 2009; Major and Lara, 2013). According to Basualto et al. (2008), the first earthquakes began ∼30 h before the first eruption on 1 May; the earthquakes were recorded by distant seismic stations located north of the volcano. Local accounts state that earthquakes were felt in Chaitén town as early as January 2008, with ∼3 earthquakes/month occurring in February and March and consistent shaking by April (**Figure 1**) (Rebecca Paisley, McGill University, personal communication, 2017). During a regional seismic survey from December 2004 to October 2005, Lange et al. (2007) recorded earthquakes clustered near Chaitén at <20 km depth. Hence the timing of the first seismic precursors at Chaitén is a major unknown factor.

Regional tectonics and mafic magma may have played a role in this eruption. Wicks et al. (2011) model the Chaitén magma as being channeled at mid-crustal levels within an ENE dipping reverse fault connected to the Liquiñe-Ofqui fault zone beneath Michinmahuida volcano ∼15 km east of Chaitén. Although no mafic magma was erupted in 2008-2009, some plagioclase cores reach An_{81} (Pallister et al., 2013), and the 9.4 ka eruption erupted mafic scoria (Major and Lara, 2013).

Merapi, Indonesia, 2010

Merapi is a highly active volcano of basaltic andesite composition. Prior to 2010, it last erupted in 2006. Its typical activity comprises periods of lava dome growth and collapse interspersed with quiescent periods. After a year of low-level precursory activity, Merapi erupted violently for 11 days from 26 October to 5 November 2010, with a series of explosions which generated devastating pyroclastic density currents (**Table 1**). Interspersed with the explosions were periods of rapid lava dome growth. A phreatomagmatic explosion initiated the eruptive sequence on 26 October, followed by explosions and then rapid dome growth with further explosions during 1–4 November. The most violent phase of VEI 4 was initiated in the early hours of 5 November, destroying the new dome and producing ash columns to 17 km altitude and long-runout pumiceous and scoriaceous pyroclastic density currents. This paroxysm was followed by a second phase of rapid dome growth on 6–8 November. Afterward, the activity declined to low levels by the end of November (Surono et al., 2012; Komorowski et al., 2013).

Clear seismic precursors began on 31 October 2009, one year before the eruption, and continued to June 2010 at a low level (Budi-Santoso et al., 2013). Precursory activity began to accelerate significantly in early September 2010, as manifested by increased inflation on 4–5 September followed a week later by a noticeable increase in volcanotectonic and hybrid earthquake occurrences (**Figure 2**). This acceleration thus occurred nearly 2 months before the eruptive activity. A third acceleration began 10–13 October, as manifested by strongly increasing inflation, rockfalls, and volcanotectonic and hybrid earthquakes. The paroxysmal 5 November eruptions were preceded by a sequence of long period earthquakes from 29 October to 3 November (**Figure 2**) (Surono et al., 2012).

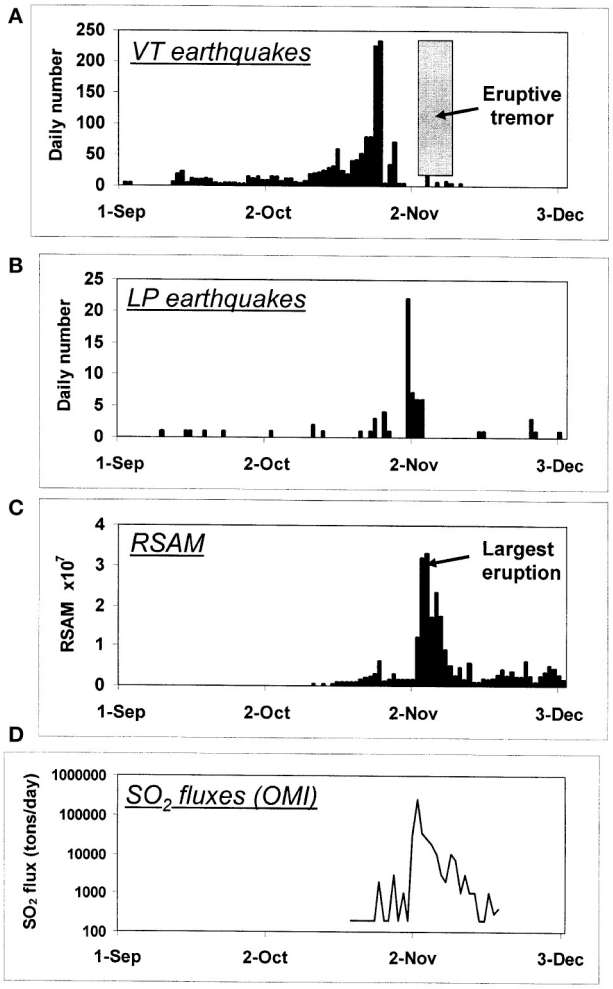

FIGURE 2 | Earthquakes and SO_2 fluxes at Merapi, September-November 2010. Note the appearance of volcanotectonic (VT) earthquakes in September 2010, their escalation in early-mid October, and their rapid decline by the end of October. Long-period (LP) earthquakes are clustered in latest October and earliest November. The paroxysmal eruptive phase during 3–5 November is associated with maximum RSAM, maximum SO_2 output, and the occurrence of eruptive tremor. Surono et al. (2012), Copyright 2012, with permission from Elsevier.

The juvenile material was both crystal-rich (Drignon et al., 2016) and volatile-rich, with melt inclusions reaching nearly 4 wt. % H_2O and ∼3,000 ppm CO_2 (Preece et al., 2014) and matrix glasses up to 6.6 wt. % H_2O (Drignon et al., 2016) (**Table 1**). The pronounced inflationary behavior in October indicates that a batch of volatile-rich magma was quickly rising to shallow crustal levels below and into the volcano, followed by its appearance on the surface as a new lava dome grew during 1–4 November. The presence of the dome allowed the shallowly emplaced magma to undergo pressurization, as shown by the long period seismic swarm of 29 October−3 November and the low SO_2 fluxes (<1,000 metric t/d) during this period, followed by the 5 November pumice-bearing paroxysmal eruption and very large SO_2 releases ($>10^5$ t/d) on 3–6 November (**Figure 2**) (Surono et al., 2012).

This highly eruptable and highly pressurized magma was sensitive to external perturbation. A series of tectonic earthquakes occurred on 3–4 November, closely followed by explosions (Surono et al., 2012). Most notably, a M4.2 regional earthquake occurred at 23:56 h local time on 4 November, followed 6 min later by the start of the 5 November eruptive sequence (Komorowski et al., 2013). Jousset et al. (2013) suggest that seismic waves from the earthquake triggered the eruption; this is very likely given that the shallow magma was volatile-rich, vesicular, and overpressured, hence fragile.

In summary, the precursory activity comprised a series of well-defined stages over the course of a year. A significant increase in unrest began 2 months before the climactic eruption, with a further increase about 3 weeks beforehand. Overpressure developed rapidly for several days immediately prior to the climactic 5 November eruption. Afterward, the activity dissipated rapidly within a month.

Mt. St. Helens, USA, 1980

Mt. St. Helens is the most active volcano of the Cascades volcanic arc. Its last activity prior to 1980 occurred in the first half of the nineteenth century, comprising explosive eruptions, lava flow activity, and lava dome growth. The 2-month sequence of events leading to the 18 May 1980 eruption reveals interesting correlations and changes with time. The first eruption occurred on 27 March 1980, and at least 13 eruptions occurred the next day (Christiansen and Peterson, 1981). Eruptions ceased temporarily on 22 April, resumed during 7–14 May, and then ceased again until the major eruption on 18 May (**Table 1**). Although these eruptions were believed to be phreatic in nature at the time (Sarna-Wojcicki et al., 1981), subsequent work by Cashman and Hoblitt (2004) demonstrated that ash deposits from the 28 March and 16 April eruptions contain juvenile glass. Hence at least some of these eruptions were phreatomagmatic, not phreatic. Between eruptions, SO_2 fluxes were less than 10 t/d, while SO_2 fluxes associated with eruptive activity were generally higher reaching 30 t/d (Casadevall et al., 1981). During this time, significant amounts of H_2S were also released along with the SO_2 (Hobbs et al., 1981).

The volcano began inflating in mid to late March 1980, with a bulge visible by early April on the north side (Lipman et al., 1981; Moore and Albee, 1981). By April and May the bulge was expanding laterally at a rate of 1.5–2.5 m/day (Lipman et al., 1981; Moore and Albee, 1981). The exact time of the initiation of inflation is not known, nor the inflation rate at early stages. The first anomalous seismicity was recorded on 15 March 1980, with a rapid increase on 22–23 March from less than 5 to 20–30 events/hour (Endo et al., 1981). The largest number of earthquakes and the greatest energy release occurred in late March and early April, followed by a general decline afterward to 18 May (Endo et al., 1981). The earthquakes were dominated by long period events (Endo et al., 1981; Hofstetter and Malone, 1986). Low-frequency tremor episodes occurred in two clusters, a stronger set from 31 March to 12 April, and a second weaker set during 7–10 May (Hofstetter and Malone, 1986).

The plinian phase of the 18 May eruption (VEI 5) lasted approximately 9 h, with discharge rates on the order of 1.9×10^7 kg/s and a DRE volume of erupted magma of ∼0.24 km^3 (Carey and Sigurdsson, 1985). The magma contained ∼40% crystals (mostly plagioclase) and up to 6.7 wt. % H_2O (Rutherford et al., 1985; Blundy et al., 2008) (**Table 1**). Over the next 6 years the volcano experienced diminishing activity, with the emplacement of a series of lava domes and associated unrest.

In summary, the substantial phreatic and phreatomagmatic activity, long period earthquake occurrences, and low-frequency tremor observed in late March and early April are likely the product of upward magma transport to shallow levels beginning at this time. Earthquake hypocenters during this time were 2–3 km deep (Endo et al., 1981). By contrast, the comparative lack of eruptions, earthquakes, and tremor in the last 4–8 days prior to 18 May indicates relative quiescence immediately before the climactic eruption.

Mt. Pinatubo, Philappines, 1991

Mount Pinatubo is a composite volcano in the Luzon volcanic arc which has erupted repeatedly and explosively in Holocene time (Newhall et al., 1996). The volcano re-activated in March 1991, and the elapsed time between initial activity and the climactic eruption was 3 months. The first earthquakes were felt by local residents on 15 March 1991, while a series of explosions on 2 April opened a northeast trending system of steaming vents (Sabit et al., 1996). The 2 April explosions were interpreted as phreatic or hydrothermal (Wolfe and Hoblitt, 1996). The steaming became focussed at three vents which were located close to the site of later lava dome extrusion in early June. RSAM values were stable from 10 to 31 May (**Figure 3A**) (Harlow et al., 1996), and cumulative earthquake totals increased at a near-constant rate from 5 April to 6 June (**Figure 3B**) (Sabit et al., 1996), although these authors did record an increase in high frequency earthquakes in early to mid May. These earthquakes were mainly situated 5 km north-northwest of the summit at a depth of 2–6 km, with a secondary cluster closer to the volcano below the vents at a depth of less than 4 km (Harlow et al., 1996). During May, steaming intensified, and progressively greater quantities of ash were emitted along with the steam. The first measurement of SO_2 flux on 13 May recorded 500 t/d (Daag et al., 1996) (**Table 1**).

The unrest changed significantly at the end of May. On 28 May, 5,000 t/d SO_2 were measured at the same time as a cluster of deep long period earthquakes and tremor were recorded on 26–28 May, interpreted by White (1996) as intrusion of basaltic magma from the deep crust or mantle. This magma arrived at the base of the dacitic reservoir on or about 2 June (White, 1996). RSAM values began to increase on 1 June compared to their stability in May (**Figure 3A**), and the concentration of high frequency earthquakes closer to the volcano became dominant and shallowed with time (Harlow et al., 1996). A second cluster of deep long period earthquakes and tremor was recorded from 31 May to 8 June, interpreted by White (1996) as a second batch of basaltic magma which moved upward. During this time SO_2 fluxes progressively declined from a high of 5,000 t/d on 28 May to a low of 260 t/d on 5 June (Daag et al., 1996), while a tiltmeter near the summit recorded inflation (Ewert et al., 1996). A lava dome appeared on 7 June and grew until at least 11 June and possibly later (Wolfe and Hoblitt, 1996). The highest

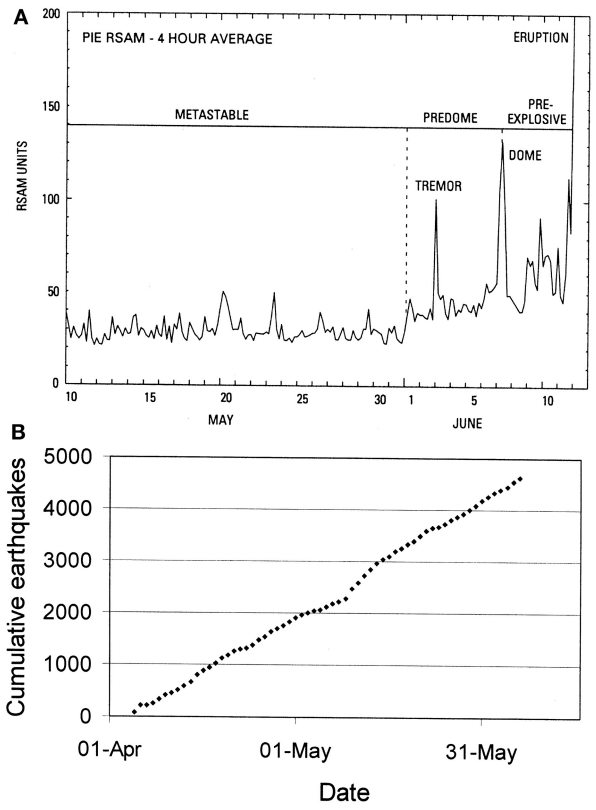

FIGURE 3 | (A) RSAM values from station PIE on Mt. Pinatubo in May-June 1991. Note the stability in May and the increases in early-mid June. From Harlow et al. (1996) and reproduced courtesy of the University of Washington Press. **(B)** Cumulative earthquake totals recorded at Yamut station on Mt. Pinatubo from 5 April to 6 June 1991. Note the steady accumulation of earthquakes during this time. Data from Sabit et al. (1996).

SO_2 flux of >13,000 t/d was measured on 10 June. Four major explosions occurred on 12–14 June, followed on 14–15 June by 13 eruptions which were progressively closer spaced in time, producing pyroclastic surges. The VEI 6 climactic eruption on 15 June began at 13:42 h local time and lasted 9 h, forming a summit caldera (Wolfe and Hoblitt, 1996). The dacite that was erupted contained 15–47% phenocrysts (Pallister et al., 1996), with ∼6.4 wt. % H_2O dissolved in the magma prior to eruption (Rutherford and Devine, 1996), and the total volume of magma erupted was 3.7–5.3 km^3 (Scott et al., 1996) (**Table 1**). After the climactic eruption, seismicity and degassing declined rapidly over the space of several weeks. By September 1991 a lake had formed in the summit caldera, and a lava dome with a volume of 4×10^6 m^3 was extruded from July through October 1992 (Wolfe and Hoblitt, 1996).

In summary, the 1991 precursory unrest at Mt. Pinatubo can be divided into two periods. The first period began in mid-March and ended in late May; it was characterized by comparatively subtle changes in the magmatic-hydrothermal system of the volcano. The second period began in late May lasting until the climactic 15 June eruption; it was characterized by a significant escalation in geophysical unrest, as well as eruptive activity which began on 7 June.

FOUR VOLCANOES WITH SLOW ACTIVITY

Soufrière Hills, Montserrat, 1989-2018

Soufrière Hills is an andesitic volcano which experienced three seismic crises at regular intervals of 30–35 years in the nineteenth and twentieth centuries (1897–1898, 1933–1937, 1966–1967) (Wadge and Isaacs, 1988), prior to the first eruption of the current cycle on 18 July 1995. Seismicity began to increase above background levels in April 1989, and earthquake swarms were first detected in January 1992 (Kokelaar, 2002). Hence volcanic unrest has been ongoing for 29 years and continues today, with steady SO_2 degassing at ∼370 t/d and stable fumarole temperatures reaching 610°C (Christopher et al., 2015) (**Table 2**). These authors have proposed that the volcano is underlain by a crustal scale magmatic plumbing system.

It is instructive to examine the period 1995–1997 during which a significant escalation of activity occurred, followed by temporary quiescence from March 1998 to November 1999 when lava dome growth resumed. This 2½ year period in 1995–1997 followed seismic unrest which had been ongoing for 6 years. The key escalatory events occurred in 1996 and 1997. At the time, the escalation was first not anticipated and then under-appreciated, in particular the transition from purely lava dome growth-collapse cycles to periods of explosive activity. Activity was initiated by a series of phreatic explosions in July-August 1995, and an oxidized lava spine appeared in the crater in late September 1995 (Sparks and Young, 2002). A lava dome began forming in November 1995, with the first major pyroclastic flows from collapse of the growing dome on 31 March 1996. A period of high dome growth and associated pyroclastic flow activity occurred in July-August 1996, followed by the first magmatic explosive eruption on 17 September 1996 after 40% of the dome collapsed (11.7×10^6 m^3) (Robertson et al., 1998). Very high levels of dome growth occurred in May–June 1997, with large collapses and large pyroclastic flows producing loss of life on 25 June. Two sequences of magmatic vulcanian eruptions occurred on 4–12 August and 22 September-21 October (Druitt et al., 2002), followed by sector collapse of the crater and a lateral magmatic blast on 26 December 1997. Water contents in melt inclusions from pumices of the 1997 vulcanian activity reveal a maximum of 6.7 wt. %, with most values 3–5 wt. % (Mann et al., 2013).

The transition from dome growth to explosive eruptions can be seen for both 1996 and 1997. For 1996, a period of enhanced dome growth, collapse, and pyroclastic flows was observed in late July until mid-August, with magma discharge rates of 3–5 m^3/s (Sparks and Young, 2002). A sequence of 85 regularly spaced hybrid earthquake swarms, with maximum RSAM values of ∼1850 at the Long Ground seismic station, occurred from 27 July until 13 August with spacings of 3–6 h (∼5 h was typical) (**Figure 4**). Although there were no tiltmeters installed at the time, the repeating seismicity was likely associated with inflation-deflation cycles similar to those observed in 1997. The seismic swarms essentially define a period of "banded tremor." These unusual seismic signals can be generated by at least two mechanisms. At volcanoes such as Nevado del Ruiz (Colombia), Etna (Italy), and Karkar (Papua New Guinea), the banded tremor

TABLE 2 | Characteristics of slow volcanic systems.

Volcano	Soufrière Hills	Turrialba	Popocatépetl	Nevado del Ruiz
Duration of unrest (years)	30	23	28	35
Date of initial unrest	April 1989	May 1996	late 1990	late November 1984
Date of first significant eruptive activity	18-Jul-1995	5-Jan-2010	21-Dec-1994	11-Sep-1985
Elapsed time between initial unrest and first eruptive activity (months)	75	164	48	∼10.5
Initial indicators of unrest	Earthquakes	Earthquakes	Earthquakes	Increased fumarolic activity, earthquakes
DRE cumulative volume of erupted magma (km^3)	1.1	Close to zero	∼0.04	<<1
Magma composition	Andesite	Basaltic andesite	Andesite, dacite	Andesite
Maximum water content of magma (wt. %)	6.7	no data	∼3	3.3
Evidence for mafic magma?	Yes	?	Yes	?
Sources of data	Christopher et al., 2015 Kokelaar, 2002 Mann et al., 2013 Sparks and Young, 2002	De Moor et al., 2016 Martini et al., 2010	De la Cruz-Reyna et al., 2008 Delgado-Granados et al., 2001 Gómez-Vazquez et al., 2016	Londoño, 2016

is likely generated by periodic injections of magmatic gases into a hydrothermal system (Martinelli, 1990; Stix and de Moor, 2018). At Montserrat, the tremor is likely the result of enhanced magma flow and pressurization in the shallow conduit system (Voight et al., 1998). Both types of banded tremor can lead to explosive eruptions, as was observed at Nevado del Ruiz, Etna, and Karkar, as well as at Soufrière Hills where the first explosive eruption occurred on 17 September 1996. Hence the July-August activity can be viewed as a harbinger of future explosive activity.

Similarly, the rapid growth of the dome in May-June 1997 heralded the later explosive activity in August. Magma discharge rates were 7–8 m^3 s^{-1} in May (Sparks and Young, 2002), and a major dome collapse of 6.4×10^6 m^3 occurred on 25 June. This event may have been close to triggering an explosive eruption, since conditions reached the effusive-explosive threshold requiring (a) an elevated magma discharge rate of 7–8 m^3 s^{-1} and (b) a large dome collapse event (Druitt et al., 2002). By contrast, the July-August 1996 activity appeared to be below this threshold, as the discharge rates and collapse volumes were smaller.

Hence, the overall activity from late 1995 to the end of 1997 is one of increasingly vigorous magma discharge and dome growth and progressively more frequent and more intense explosive episodes. Prior to the explosive episodes in 1996 and 1997, there were escalations in activity which in retrospect indicated that the volcano was capable of transitioning from effusive to explosive activity.

Turrialba, Costa Rica, 1996–2018

Turrialba is an andesitic volcano which last erupted in 1864–1866. The volcano began to show signs of new unrest in 1996. During the past 22 years Turrialba has exhibited a remarkable and progressive re-activation. The first anomalous seismicity was recorded in late May 1996 (GVN Bulletin, 1996) (**Table 2**). The initial several years of unrest were dominated by hydrothermal activity, while the system has become progressively more magmatic with time. Martini et al. (2010) have divided the volcano's activity into three periods, the first from 1996 to 2000 when the system was dominated by low fumarolic temperatures and hydrothermal gases, the second from 2000 to 2006 which represents a period of structural opening with increased seismicity, declining pH of fumaroles, and the appearance of magmatic gases such as SO_2, and the third beginning in 2007 and continuing today with clear evidence of magmatic input including volcanotectonic, long period, and hybrid seismic swarms, high SO_2 fluxes, new high-temperature vents, explosions beginning in 2010, ash emissions in 2014–2017 with possibly juvenile glass, and lava bombs in early 2017.

Although SO_2 fluxes have not been measured on a continuous basis, the data that are available paint an interesting picture. SO_2 was first detected in fumaroles in November 2001, and small but measurable SO_2 fluxes were observed in 2002 (Martini et al., 2010). By 2008 fluxes were 500–1,000 t/d which continued until the second half of 2009 when fluxes increased significantly to levels of 3,000–4,000 t/d. These levels generally were maintained in 2010 with lowered fluxes in 2011 (typically >2,000 t/d) and 2012 (< 2,000 t/d) (Conde et al., 2014). In 2014 most fluxes were <1,000 t/d, then increased late in the year and maintained in 2015 with fluxes typically 1,000–2,000 t/d including both lower and higher values (De Moor et al., 2016). This summary highlights two key points: (a) the first SO_2 signals occurred in late 2001, about a year after the pH of fumarole condensates started decreasing (**Figure 5**) (Martini et al., 2010); (b) SO_2 fluxes have been elevated since at least 2008, a clear indication of a magmatic component.

Eruptive activity has likewise progressed in a stepwise manner. The first explosions opened a high temperature vent (300–600°C) on 5 January 2010, followed by further explosions in January 2012

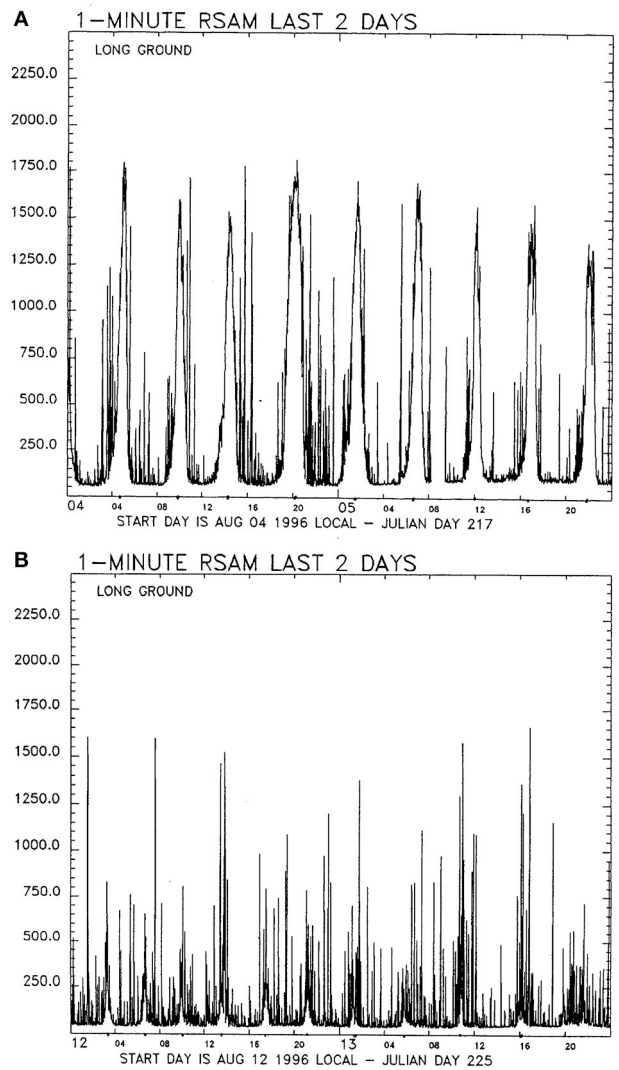

FIGURE 4 | Banded tremor at Soufrière Hills volcano in August 1996. The vertical scale is RSAM units at the Long Ground seismic station ∼2 km northeast of the volcano's summit. **(A)** Tremor on 4–5 August. Note the maximum RSAM value of 1800 and the ∼5-h spacing of tremor bands. **(B)** Tremor on 12–13 August. The maximum RSAM has declined to 1650, and the tremor bands are now spaced at intervals of 3–4 h. Data kindly provided by the Montserrat Volcano Observatory.

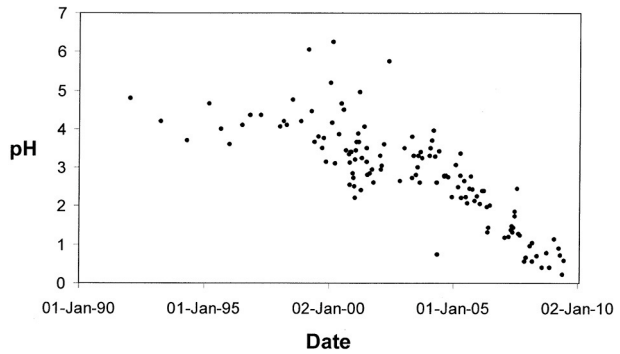

FIGURE 5 | Values of pH from West crater fumaroles at Turrialba, 1992–2009. Note the relatively stable and high values from 1992 until 2000, the gradual decline from 2000 to 2004, and the steep decline since then. Martini et al. (2010), Copyright 2010, with permission from Elsevier.

opening a second vent at 500–800°C. SO_2 fluxes reached ∼5,000 t/d immediately after the 2010 vent opening (Campion et al., 2012). These are the highest fluxes yet observed at Turrialba. A more vigorous period of eruptive activity began 29 October 2014 with the emission of possibly juvenile magma (De Moor et al., 2016). Further explosions, ash emissions, and incandescence were recorded from late 2014 to the present day, with particularly vigorous periods of ash venting events during 8 March−18 May 2015 (De Moor et al., 2016), May–June 2016, and February 2017.

To summarize, the re-activation at Turrialba has been remarkably slow and progressive in nature. The observations and data from Turrialba indicate that a volume of magma, estimated at ∼0.3 km^3 by De Moor et al. (2016), is resident in the shallow plumbing system beneath the volcano. Yet it is also clear that this magma has difficulty reaching the surface. Its volume may be too small, it may be too viscous, degassed, and crystallized, and/or it is being efficiently contained by a near-surface hydrothermal seal.

Popocatépetl, Mexico, 1990–2018

Popocatépetl is a 5,452 m stratovolcano located near Mexico City. In the last 23,000 years the volcano has experienced at least 7 plinian eruptions (Macías and Siebe, 2005). In the past 500 years the volcano has had more moderate activity comprising explosions, dome growth, and dome destruction episodes. This record suggests that the volcano has experienced episodes of both fast and slow activity. The current unrest began in 1990 when anomalous volcanotectonic earthquakes beneath the volcano were first recorded (De la Cruz-Reyna et al., 2008) (**Table 2**). These authors recognized four periods of precursory seismicity prior to the first eruption on 21 December 1994. An initial pulse of seismicity in late 1990 defining Phase I was followed by a period of steadily accelerating seismicity from early 1991 through the first quarter of 1994 (Phases II and III), with a subsequent lull before another increase in seismicity leading up to the 21 December eruption (Phase IV) (**Figure 6**). The pH of the crater lake began to decline in 1992, followed by increases in lake water temperatures in 1993 and 1994. Fumarolic activity increased in 1993, and the first COSPEC measurement in February 1994 revealed an elevated SO_2 flux of ∼1,200 t/d (De la Cruz-Reyna et al., 2008). Ash emissions have occurred since 1994; ash emitted in 1997–1998 contained olivine of $Fo_{84–86}$, indicating involvement of mafic magma (Witter et al., 2005). A lava dome was emplaced in the crater on 25 or 26 March 1996 (Delgado-Granados et al., 2001; De la Cruz-Reyna et al., 2008). This was the first unequivocal indication of magma since the volcano had started its re-activation in early 1990 more than 6 years earlier. Magmas erupted in 1997-1998 reveal pre-eruptive water contents of ∼3.3 wt. % (Witter et al., 2005).

From 1996 to 2015 a total of 38 episodes of lava dome growth and destruction occurred (Gómez-Vazquez et al., 2016), and this

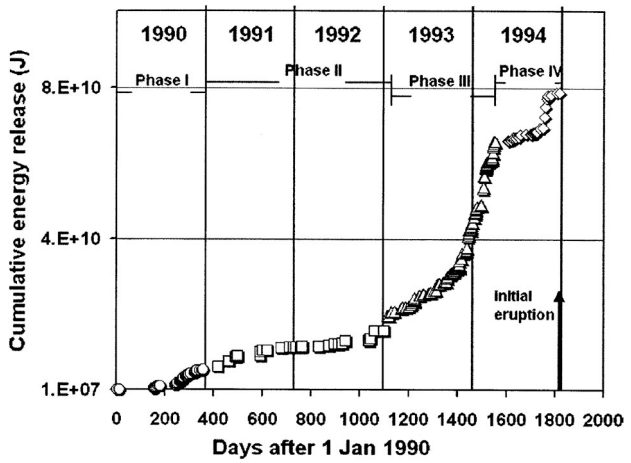

FIGURE 6 | Cumulative energy release from volcanotectonic earthquakes recorded at Popocatépetl, 1990–1994. Note the rapid increase in energy release from late 1993 to early 1994. De la Cruz-Reyna et al. (2008), Copyright 2008, with permission from Springer.

activity has continued in 2016–2017. Small domes have grown repeatedly within the enclosed summit crater. Once a dome is emplaced, it is typically destroyed by a vulcanian eruption. A number of accelerations and decelerations have occurred in terms of cumulative lava volumes and cumulative number of domes, most notably a period of acceleration during 2000–2003 and a quiet period during 2003–2011. The most intense activity occurred in December 2000, with strong harmonic tremor followed by extrusion rates of ∼28.5 m^3/s emplacing a lava dome that was destroyed by subsequent explosions in December 2000–January 2001. The 22 January 2001 eruption also generated pyroclastic flows (Gómez-Vazquez et al., 2016).

Popocatépetl has released enormous amounts of SO_2 during this unrest. Delgado-Granados et al. (2001) demonstrated that SO_2 emissions prior to dome growth were typically 2,000–3,000 t/d, with enhanced degassing during the first half of 1995 as shown by maximum fluxes of ∼9,000 t/d accompanied by a high degree of variability (<1,000 to 9,000 t/d). This was followed by a decline to <1,000 t/d by the end of 1995. Subsequent dome growth and explosive activity beginning in 1996 were associated with much higher SO_2 fluxes, typically 9,000–13,000 t/d. During this period, fluxes were again highly variable, from a low of <2,000 t/d to a high of nearly 40,000 t/d.

In summary, unrest at Popocatépetl has been characterized by two main phases, an initial period of activity from 1990 to 1996 followed by repeated dome growth and destruction cycles from 1996 to today. These cycles, now ongoing for more than 20 years, suggest a self-regulating mechanism, likely controlled by the volatile content of the magma and its ability to outgas (Gómez-Vazquez et al., 2016). These authors have speculated upon the possibility of more intense activity, e.g., a sustained plinian eruption instead of the short-lived vulcanian eruptions observed. Such an event could be generated by a larger batch of magma producing a larger dome, a magma richer in gas, or both.

Nevado del Ruiz, Colombia, 1984-2018

Nevado del Ruiz is a glacier-clad andesitic volcano 5,321 m high located in the Cordillera Central of the northern Andes. The volcano has erupted numerous times during the Holocene. A new period of unrest began in late November 1984 when fumarolic activity began increasing (Hall, 1990). An eruption on 13 November 1985 generated large lahars which killed more than 23,000 people. The volcano presents a remarkable case of extreme unrest coupled with a general lack of eruptive activity.

The cataclysmic lahar-generating 13 November 1985 eruption released a small volume of magma (3.9×10^7 m^3 DRE) (Naranjo et al., 1986), while subsequent eruptions have emitted significantly less material. The maximum pre-eruptive water content in magma ejected on 13 November 1985 is 3.3 wt. %, as revealed by melt inclusion analyses (Stix et al., 2003). Although the level of activity has varied with time during the past several decades, it has generally maintained a high level of unrest, as manifested by elevated seismicity and SO_2 emissions (**Table 2**). The unrest has extended over a wide region encompassing a number of volcanic centers; starting in 2007, this region began experiencing renewed activity (Londoño, 2016). At Cerro Machín 50 km south of Ruiz, geochemical indicators including SO_2, $^3He/^4He$, CO_2, and radon started increasing in 2007, while at Cerro Bravo ∼20 km north of Ruiz, deep long period seismic events and elevated radon and CO_2 concentrations were noted in 2008 (Londoño, 2016). At Ruiz, deformation was first noted in 2007, while seismicity and SO_2 fluxes started increasing in 2010, with SO_2 reaching levels in excess of 20,000 t/d in 2012 associated with small eruptions in May and June of that year. The elevated deformation eventually led to the emplacement of a lava dome in September 2015 (Londoño, 2016).

The region is complex structurally and magmatically. A series of large-scale faults, mainly trending northeast-southwest, intersect the volcano and adjacent region. A shallow magmatic system is present at a depth of less than 5 km, based upon petrologically measured magmatic water contents (Stix et al., 2003) and elevated V_p/V_s seismic signatures interpreted as gas-bearing magma (Vargas et al., 2017). This part of the magmatic plumbing system is the direct cause of the unrest witnessed during the past 33 years. However, there are a number of lines of evidence showing that this shallow system is underlain by at least one additional reservoir at mid-crustal to lower-crustal depths, and there may in fact be multiple reservoirs extending to the mantle. Hence Nevado del Ruiz is an excellent example of a crustal-scale magmatic system (Sparks and Cashman, 2017). Lundgren et al. (2015) have modeled the deformation since 2011 to be sourced at ∼14 km, while Londoño (2016) propose magma sources which are in the deep crust and uppermost mantle (20–40 km deep). Stix et al. (2003) propose that the shallow magmatic system is periodically replenished by volatile-rich magma from these deep sources. This is consistent with the seismic tomography of Vargas et al. (2017), in which the high V_p/V_s shallow magma results from decompression and degassing of magma rising from deeper levels. Londoño and Kumagai (2018) have demonstrated that regions of both high V_p/V_s and low V_p/V_s were accentuated in 2015–2016 relative to 2000–2006.

Such anomalies appear to be the result of new magma which has been intruded into the shallow plumbing system since 2010 (Londoño and Kumagai, 2018). Hence the plumbing system is open to inputs of magma; given the presence of regional faults intersecting the volcano, it is likely also open in a structural sense as well (Kumagai et al., 2017).

The regional plumbing system appears to be more open in certain locations than others. At Nevado del Ruiz, gas and magma can reach the surface, possibly aided by regional faults. Relative to Ruiz, Cerro Machín and Cerro Bravo volcanoes represent systems which are structurally open (e.g., elevated radon and $^3He/^4He$) but magmatically closed (no eruption has yet occurred). A crucial short-term question is the process or processes capable of opening these two systems, leading to hazardous activity including eruptions.

DISCUSSION

The eight volcanoes described above provide clear illustrations of fast and slow behavior. There are other systems which show aspects of both. My purpose here is to show that many systems activate on very short timescales of months or less, while others activate over years to decades. Using the case histories above, I now address four elements important for understanding these two types of behavior: (1) their commonalities; (2) the nature of the shallow magmatic-hydrothermal plumbing systems; (3) their grouping into closed vs. open systems; and (4) a way forward to help understand their behavior and forecast eruptions.

Common Behavior of Volcanoes With Fast Activity

The four fast systems examined here have three principal commonalities. First, all had elevated volatile contents prior to eruption. All four systems had water contents of at least 4 wt. %. In the cases of Merapi, Mt. St. Helens, and Pinatubo, the highest measured water contents approach 7 wt. %, and it is possible that Chaitén magmas contained similarly high H_2O. These very high water contents explain the high levels of explosivity of these systems, as witnessed in the paroxysmal eruptions, as well as the efficient extraction of magma from the reservoirs during the eruptions. Furthermore, a separate volatile phase was likely present in magma beneath Pinatubo and Mt. St. Helens prior to the climactic eruptions (Pallister et al., 1992; Westrich and Gerlach, 1992). Such a volatile phase may be a common occurrence and likely contributes to overpressure, explosivity, and magma extraction.

Second, the high volatile contents likely aided magma ascent. For all four systems, the rise of magma appears to have been rapid on timescales of several months or less. At Mt. St. Helens, the intense eruptive activity, seismicity, and deformation observed in late March - early April 1980 suggest that magma was rising actively and rapidly at this time. Small amounts of magma were already being erupted by 28 March (Cashman and Hoblitt, 2004), 1 day after the first eruption and only 2 weeks after the first signs of re-activation. At Mt. Pinatubo, intrusion of mafic magma beginning in late May 1991 suggests that the dacitic magma was mobilized and erupted in 3 weeks or less. Chaitén and Merapi also appear to share these very short timescales.

Third, the timescales of de-activation after the climactic eruptions also appear to be fast. Activity ceased at Chaitén and Pinatubo less than 2 years after the climactic eruptions, while at Merapi the decline in activity was an order of magnitude faster, effectively ceasing a month after the paroxysmal 5 November 2010 eruption. Only Mt. St. Helens had protracted lava dome activity lasting 6 years after the 18 May 1980 eruption.

Common Behavior of Volcanoes With Slow Activity

Pre-eruptive water contents in magmas emitted from Soufrière Hills in 1997 were typically 3–5 wt. %, with a maximum of 6.7 wt. % (Mann et al., 2013). Pre-eruptive water contents at Popocatépetl in 1997–1998 and at Nevado del Ruiz in 1985 did not exceed 3.3 wt. % (Stix et al., 2003; Witter et al., 2005). These values are generally lower than water contents for the fast volcanic systems discussed above, although there is some overlap in the case of Soufrière Hills. The material sampled for the Soufrière Hills water analyses came from the most explosive activity observed to date, which may partly explain why several melt inclusions contained high water contents.

Soufrière Hills and Turrialba have both shown progressive and unanticipated increases in activity that in retrospect were highly systematic with time. In the case of Soufrière Hills, the process of ramping up occurred over a period of about 2 years, starting with sluggish dome growth in November 1995 and ending with intense explosive activity in December 1997. For Turrialba, the activity increase occurred over two decades, i.e., an order of magnitude longer than at Soufrière Hills. The ramp-up at Turrialba may not yet be complete. The two systems exemplify behavior which is extremely difficult to forecast because the specific, individual changes have occurred in an irregular fashion over an extended period of time. Recognizing such progressive increases in activity as they are occurring is a major future challenge for scientists.

Turrialba and Popocatépetl illustrate how some volcanoes are progressively opened in a structural sense, as manifested by seismicity and degassing. The seismicity results from fracturing and opening of country rock above magma, allowing progressively more degassing to occur with time. At Turrialba, this opening process occurred over 14 years from mid-1996 when the first anomalous seismicity was observed to early 2010 when the first major explosion occurred. At Popocatépetl the process of opening occurred during 5 years from the first anomalous seismicity in 1990 to the appearance of the first lava dome in March 1996. This process may partly explain the low water contents in magmas erupted from Popocatépetl in 1997 and 1998 (Witter et al., 2005).

The Magmatic-Hydrothermal Plumbing System

Magmas associated with fast activity are generally mobile in the crust as a result of elevated temperatures and high volatile contents, and erupted magma volumes can exceed 1 km^3. By

contrast, magmas associated with slow activity are not easily erupted. They appear to be rheologically sluggish, with variable gas contents. These factors partly account for the comparatively small amounts of magma erupted from these systems. The slow-acting volcanoes examined here have each emitted ∼1 km^3 of magma or less during their extended unrest.

The magmatic holding systems may likewise differ significantly. Fast volcanic systems commonly have well-defined magma reservoirs at one or more levels in the crust, allowing magma to be first stored and then evacuated in an efficient manner. Slow volcanic systems may not have a principal reservoir; instead, magmas may be transported and stored through a complex network of dikes, sills, and other small spaces and cracks (Stix et al., 2003). Systems such as these have large surface areas which promote cooling, degassing, and magma crystallization instead of eruption. Hence the magmas are viscous, lack buoyancy, and have difficulty erupting. The principal manifestation of magmatic activity in these cases is the intense degassing and low frequency seismicity.

Sparks and Cashman (2017) propose a model whereby magmas beneath episodically active volcanoes are stored at different crustal levels from the Moho to near the surface. During periods when a volcano is inactive, lenses of melt-rich magma at a range of depths are unconnected; during re-activation, the lenses connect to allow upward migration of melt-rich magma. Volcanoes with fast activity may be associated with such periods of upward migration. Volcanoes with slow activity appear to be associated with (a) fewer connected lenses and (b) melt-poor magmas. However, both types appear capable of sustaining crustal-scale magmatic systems through the entire crust. Such a model has been proposed for Mt. St. Helens, a fast system (Pallister et al., 1992; Blundy et al., 2008), while slow systems include Soufrière Hills (Christopher et al., 2015) and also Nevado del Ruiz where the seismic and petrologic data provide a strong case for multiple magma reservoirs through the crust.

A hydrothermal system is commonly present between the shallow magmatic system and the surface. During times of quiescence, the hydrothermal system may seal the magmatic system by precipitation of silica and clays. During times of activity, the seal may be breached by rising magma, allowing strong degassing to occur at the surface. The influence that the hydrothermal system exerts on the magmatic system largely depends on its size. If the hydrothermal system is large relative to the magmatic system, it can absorb magmatic volatiles such as SO_2 and HCl and also potentially quench subsurface magma. If the hydrothermal system is comparatively small, the magmatic system will efficiently dry it, allowing increased magmatic degassing to occur at the surface. At Mt. St. Helens, the hydrothermal system likely absorbed substantial SO_2 prior to 18 May 1980, resulting in the very low SO_2 fluxes that were observed prior to the climactic eruption (Doukas and Gerlach, 1995; Symonds and Gerlach, 1998). At Turrialba, the hydrothermal influence has waxed and waned over the course of many years, becoming generally less significant with time (De Moor et al., 2016).

Injections of more mafic magma from deep levels can perturb systems at various timescales as the mafic magma interacts with resident magma. At Pinatubo, the interaction was rapid and timescales extremely short (days to weeks). At Soufrière Hills and Popocatépetl, the accelerating behavior seen at both systems was likely driven by mafic magma inputs on long timescales (years). The manner by which an introduced mafic magma influences a magmatic system, including surface activity and eruptions, depends upon its volume, the depth of interaction within the crust, and its volatile content. A small-volume injection will likely be quenched, while a large volume or multiple injections will drive eruptions. If magma mixing occurs at shallow crustal levels, the response should be felt rapidly, while deeper interactions at mid-crustal levels (10–20 km) will result in slower responses. A water-poor magma will tend to stall in the crust or at the base of the shallow magma reservoir (Wiebe, 1994), while a water-rich mafic magma will be buoyant and mobile, promoting magma interactions with and volatile transfer to resident magma.

Closed and Open Systems

Although volcanoes with fast activity are commonly open to magma inputs from deeper levels, many can be considered closed systems from the top of the shallow magma reservoir to the surface. This appears to have been the case for Chaitén, Mt. St. Helens, and Mt. Pinatubo prior to their climactic eruptions. By contrast, the conduit at Merapi was generally open, except immediately prior to the paroxysmal 5 November 2010 eruption when new lava closed and sealed the shallow plumbing system during 1–4 November. These magmas are extremely volatile-rich with resulting low viscosities. In many if not all cases, the magmas contain free gas in the form of bubbles dispersed within the magma. They are thus highly overpressured systems, and when they erupt, the extreme depressurization and vesiculation of the mobile magma lead to efficient and short-lived magma extraction, hence short eruptions. This behavior can be seen for the four fast systems examined here, as well as many others. Despite a range of magma volumes from ∼4 to 5 km^3 for Pinatubo to <1 km^3 for Merapi, their behavior in this regard is similar.

Slow volcanic systems represent systems that are open between the shallow magmatic system and the surface, as well as open to magma inputs from deep levels. The opening process begins when magma first starts to move upward, before any eruptions occur. Slow upward movement of magma causes intense fracturing in rock above, manifested by volcanotectonic earthquakes. Regional fault systems intersecting the volcano may enhance the opening process. Distal volcanotectonic earthquakes are generated along these fault systems as magma rises beneath the volcano (White and McCausland, 2016). The fracturing and faults increase permeability and allow the decompressing magma to degas freely, thereby reducing pressure on the system. The degassing also stiffens the magma rheologically by crystallization and less dissolved gas in the melt, both of which increase magma viscosity. This mechanism of opening is well-illustrated by the pattern of volcanotectonic earthquakes observed at Popocatépetl between 1990 and 1996 prior to the

first arrival of lava at the surface (**Figure 6**). Exponential increases in earthquakes and seismic energy in 1992–1994 were likely the result of both new fractures and increased fracture densities as magma slowly made its way upward (De la Cruz-Reyna et al., 2008). Elevated SO_2 fluxes of 2,000–3,000 t/d in 1994-1996 showed that the plumbing system beneath the volcano had become comparatively open. Once lava appeared at the surface in March 1996, SO_2 fluxes increased to 9,000–13,000 t/d (Delgado-Granados et al., 2001), demonstrating that at this point forward the system was fully open and the magma fully decompressed.

Perhaps the fundamental measure of whether a system is closed or open is the rate at which magma is emplaced at shallow crustal levels (<5 km). If magma is emplaced quickly (days to months), there is little time available to (a) fracture the crust above the magma to increase permeability and (b) degas the magma. As a result, large overpressures develop in the shallow, volatile-rich magma caused by decompression, vesiculation, and crystallization, leading rapidly to large explosive eruptions. By contrast, if slowly emplaced, magma will open the system progressively and efficiently through fracturing. The magma also will lose gas in the subsurface as it slowly rises (Moran et al., 2011; White and McCausland, 2016), and the fractured crust will aid the degassing process. Hence the magma may stall at shallow levels, and eruptions will be small and infrequent. For caldera systems, Sandri et al. (2017) suggest that the residence time of new magma in a shallow reservoir determines the probability of eruption. Short residence times limit degassing and promote eruption, while longer residence times promote degassing and limit eruption.

A further potential difference between closed (fast) and open (slow) systems is the nature of the magma body or bodies that are emplaced. A batch of mobile magma that moves rapidly upward may be emplaced as a single, well-defined, coherent body. A magma that moves slowly may seek a number of pathways as it rises, such as cracks, fractures, and faults in the crust, generating complex sill-dyke systems and resulting in a less focused and more diffuse magma plumbing system. If such differences do exist, they could be potentially imaged by seismic tomographic techniques.

New Approaches for Eruption Forecasting

Figure 1 illustrates activity at seven fast volcanic systems before and after their climactic eruptions. The dataset is small but potentially useful for forecasting purposes. Of the seven volcanoes shown, two (Merapi and El Chichón) exhibited subtle precursors 1-2 years before their paroxysmal eruptions. All seven volcanoes, including Merapi and El Chichón, exhibited a period of 1–4 months' precursory activity prior to their large eruptions. How reliable is this 1–4 month precursory window? For the four fast systems examined here, there is considerable uncertainty for Chaiten (1 day vs. ∼3 months vs. several years?), two timescales of precursory unrest for Merapi (1 year, ∼2 months), and well-defined periods of 2 and 3 months for Mt. St. Helens and Pinatubo, respectively. The data from these and other fast systems shown in **Figure 1** may provide useful constraints on this precursory timescale. The timescale of several months is short and may indicate when magma begins moving upward into the shallow plumbing system. We need to look carefully for precursory data on a timescale of 3 months or longer, as was done for Merapi and also for El Chichón volcano in Mexico. At El Chichón, clear seismic precursors were observed starting on 1 March 1982, 1 month prior to the March-April 1982 explosive eruptions (Jiménez et al., 1999). The eruptive phase lasted 1 week, followed by a return to low-level seismicity after about a month (Espíndola et al., 2006). This is classic "fast" behavior. However, anomalous seismicity was observed retrospectively starting in January 1980, more than 2 years prior to the eruptions. This seismicity comprised 78 hybrid events which were recorded by the Chicoasen network between 1 January 1980 and 28 February 1982 (Jiménez et al., 1999). Within this network, the station closest to the volcano (TPN) was 27 km distant, suggesting that the total of 78 events is a minimum value. Hence, if such longer-term signals are present, then the short and limited window of decision making that is available prior to a large eruption can be expanded to include additional preparatory time before rapid magma ascent to the surface begins.

For volcanoes with slow behavior, it can take years (e.g., Soufrière Hills) to decades (e.g., Turrialba) before the first explosive activity is recorded. At Soufrière Hills, six years of seismicity occurred before the first eruption in July 1995. At Turrialba, there was no clear evidence of magma at shallow levels for many years. Elevated SO_2 fluxes were first recorded in 2007, possibly juvenile ash was first noted in 2014, and lava bombs were first observed in 2017. Similarly at Popocatépetl, there was a period between 1990 and 1996 when it was not clear if the unrest was being caused by magmatic renewal. At Nevado del Ruiz, renewed activity began in 2010, and a small lava dome first emerged at the surface in 2015. Hence for these types of volcanoes, the level of uncertainty regarding the magmatic contribution can remain high for an extended period of time.

Before and during initial unrest, the key questions that need to be answered for both fast and slow behavior are the following. (1) Is new magma present beneath the volcano, and if so, at what level or levels? (2) What is the volume of new magma? (3) Will the new magma rise to the surface, and if it does, how fast will this process be? To answer these questions, it may be possible to apply some recently developed approaches, namely (1) examining early phreatic eruptions and characterizing early degassing, (2) using seismic velocities to identify new bodies of magma, and (3) calculating intruded magma volumes by means of precursory volcanotectonic seismicity. These are discussed in turn in terms of fast and slow behavior.

Phreatic Activity and Associated Gases

The early stages of unrest are commonly characterized by phreatic eruptions. Such activity has occurred at both fast systems (e.g., Mt. St. Helens, Pinatubo) and at slow systems (e.g., Soufrière Hills, Turrialba). Such events may hold important clues to the subsequent behavior of an activating system. In particular, is there a magmatic component to the phreatic eruption or eruptions at the earliest stages of activity? Are the released gases purely magmatic, purely hydrothermal, or a

mixture of the two? By definition, phreatic eruptions are those that contain no solid juvenile material. They may be caused by meteoric water percolating downward to hot rocks; they also may be caused by injection of hot gases from a deeper magma body. At Mt. St. Helens measurably higher SO_2 fluxes were associated with precursory eruptions compared to periods of quiescence, suggesting that new magma was providing some heat and gas to the system at early stages. A retrospective examination of ash from the phreatic eruptions also showed the presence of glassy juvenile material (Cashman and Hoblitt, 2004), although the presence of glass is not always proof of new magma (see Pardo et al., 2014). A recent study by White and McCausland (2016) revealed a strong link between the occurrence of phreatic eruptions and peaks in seismic moment generated by distal volcanotectonic earthquakes associated with faults on and near a volcano. This relationship was interpreted as rising magma that was able to pressurize aquifer systems, thereby reducing the effective normal stress on the faults to cause the earthquakes.

The gases associated with these early phreatic eruptions can be assessed for their degree of magmatic input by using gas ratios (Aiuppa et al., 2005; Shinohara, 2005). For a volcano with fast activity, two scenarios can be envisaged. First, the CO_2/SO_2 and H_2S/SO_2 ratios measured in phreatic gases may be relatively low (CO_2/SO_2 1–5, H_2S/SO_2 ~0), clearly indicative of magmatic gases and a magmatic component at an early stage (Aiuppa et al., 2017). Such gases should have measurable SO_2 fluxes. Second, $CO_2/(SO_2+H_2S)$ and H_2S/SO_2 are comparatively high initially [$(CO_2/(SO_2+H_2S)$ >10, H_2S/SO_2 1–2] from partial absorption of magmatic SO_2 by the hydrothermal system (scrubbing) (De Moor et al., 2016; Aiuppa et al., 2017), but will decrease rapidly to magmatic values due to drying of the hydrothermal system, which is controlled by the volume of the magma body and the rate of intrusion.

At fast systems, clear precursors appear several months prior to paroxysmal eruptions, as discussed above. Gas ratios may have the potential to provide useful information on longer precursory timescales (e.g., 1–2 years) prior to eruption. Subtle changes in CO_2/SO_2 and H_2S/SO_2 may be occurring during this time interval. Furthermore, the CO_2/H_2S ratio could be useful if no SO_2 is present. Magmatic CO_2 is not scrubbed like SO_2, while H_2S represents hydrothermal input. Therefore, small increases in CO_2 and CO_2/H_2S in fumarolic gases could be indicative of the presence of new magma, which may be residing at comparatively deep levels in the crust before it rises to shallower levels.

For a volcano with slow behavior, the key parameters are (1) the role of hydrothermal vs. magmatic gases and (2) periodic magma intrusions. Two situations can be envisaged. First, in the case of progressively increasing activity on timescales of years (e.g., Soufrière Hills, Turrialba), CO_2/SO_2 and H_2S/SO_2 should show decreasing values as magmatic gases become dominant relative to hydrothermal gases. Second, periods of discrete intrusion, which help maintain the system's activity and longevity, will be accompanied by an increase in CO_2/SO_2 as CO_2-rich magma from deep levels is introduced into the shallow plumbing system. This was observed twice at Turrialba in 2014-2015 prior to periods of ash emissions (De Moor et al., 2016).

Seismic Tomography

A series of recent seismic tomographic studies have applied V_p/V_s ratios to imaging magma bodies (e.g., Patanè et al., 2006; Koulakov et al., 2013; Vargas et al., 2017; Londoño and Kumagai, 2018). The studies have involved taking tomographic snapshots at different times, thus allowing 4D imaging of a volcano. Clear V_p/V_s anomalies have been observed that change over time. At Etna, low V_p/V_s ratios associated with the 2002-2003 eruption were interpreted as intrusion of volatile-rich basaltic magma (Patanè et al., 2006). At Mt. Spurr in Alaska and at Nevado del Ruiz, high V_p/V_s ratios were associated with volatile-bearing magma bodies (Koulakov et al., 2013; Vargas et al., 2017). At Ruiz, the anomalies waxed and waned over the course of several years (Vargas et al., 2017; Londoño and Kumagai, 2018). Such temporal changes in V_p/V_s potentially could be used to track new magma inputs, as well as the development of free gas (i.e., a separate volatile phase) in a magma and the resulting pressurization. For example, Husen et al. (2004) identified a body of low V_p and low V_p/V_s at ~2 km depth which was located along the northwestern margin of Yellowstone caldera (also see Huang et al., 2015). They interpreted this anomaly as a body of free gas, possibly CO_2 from degassing magma at deeper levels. The results of Londoño and Kumagai (2018), which reveal anomalies of both elevated and depressed V_p/V_s, may be significant in this regard.

This approach may be useful for both fast and slow activity. What is required is first good baseline V_p/V_s data as a function of time, and second adequate time slices, i.e., at least monthly analyses for a restless volcano. The data can be applied in three ways. (1) Information could be obtained at an early stage ($\geq$1 year) before obvious precursors appear. For example, ascent, decompression, and degassing of CO_2-rich magma from the mantle or deep crust could be recorded simultaneously by elevated V_p/V_s ratios measured by the seismic network and also by elevated CO_2/H_2S measured at the surface. (2) For volcanoes with fast behavior, V_p/V_s anomalies could change rapidly on timescales of weeks and shallow with time. The seismic data could potentially be usefully integrated with the gas ratio data. (3) For slow behavior, changes in V_p/V_s could help identify periods of shallow magma intrusion, aided by increasing CO_2/SO_2 gas ratios. The seismic tomographic work of Londoño and Kumagai (2018) is a major step forward in this direction.

Precursory Volcanotectonic Seismicity and Deep Long Period Events

During magmatic rejuvenation, swarms of precursory volcanotectonic earthquakes occur along faults which pass near or intersect the volcano. Peaks in energy release from these earthquakes are commonly associated with phreatic explosive activity, suggesting that pressurized aquifers help trigger the earthquakes (White and McCausland, 2016). These authors have discovered a simple, elegant relationship between cumulative seismic moment of the precursory earthquakes and the magma volume which is intruded into the volcano. This relationship is expressed as $\log_{10}V = 0.71\ \log_{10}\sum M - 5.32$ where V is magma volume in m^3 and M is seismic moment in N m. The relationship can be used in two ways which are shown

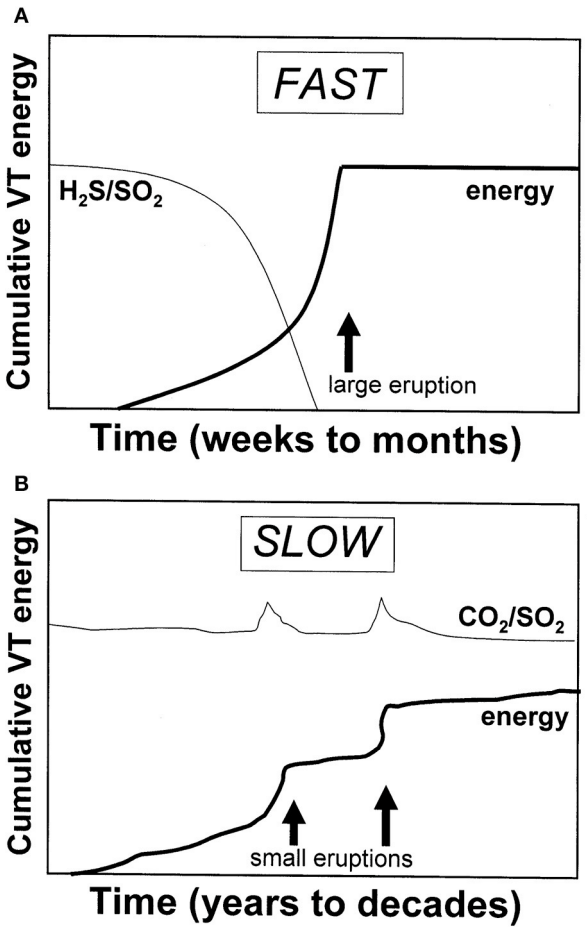

FIGURE 7 | Schematic representations of cumulative energy release of distal volcanotectonic earthquakes for fast and slow volcanic systems. Note the difference in scale for the horizontal axis between **(A)** (weeks to months) and **(B)** (years to decades). In **(A)** the H_2S/SO_2 ratio of gases is plotted with the earthquake cumulative energy, while in **(B)** the CO_2/SO_2 ratio of gases is plotted with the cumulative energy. Plot based upon work by White and McCausland (2016) and De Moor et al. (2016).

schematically in **Figure 7**. (1) For fast behavior, the rate of cumulative energy release as a function of time should be high and accelerating as magma rises rapidly, with the total energy release proportional to the magma volume involved (White and McCausland, 2016). (2) For slow behavior, increases in cumulative energy release at specific times can identify episodes of shallow magma intrusion. The volume of magma involved is indicated by the cumulative energy peaks. Furthermore, it may be possible to relate these cumulative energy data with V_p/V_s and gas ratios for deeper insight. For example, **Figure 7A** shows rapidly declining H_2S/SO_2 as rising magma dries the hydrothermal system. **Figure 7B** shows positive peaks in CO_2/SO_2 which are indications of shallow magma intrusion (De Moor et al., 2016).

As a final point, White (1996) used the first appearance of deep (>28 km) long period earthquakes beneath Mt. Pinatubo in late May 1991 to record the time at which mafic magma first ascended from deep levels and then began interacting with the dacitic magma reservoir beneath the volcano. Such earthquakes and their changing character with time appear extremely useful in terms of forecasting activity and eruptions at various timescales for both fast and slow volcanic systems. At Pinatubo, the timescale was extremely short on the order of 1–3 weeks, emblematic of the volcano's fast behavior. For a volcano exhibiting slow activity, periodic injections of mafic magma from deep levels could be signaled by deep long period earthquakes. In some cases, these signals could appear well in advance of other signs of unrest for both types of volcanoes.

A Conceptual Model

The approaches discussed above have been synthesized into a schematic fashion which shows the rapid intrusion and rise of magma beneath a fast volcanic system (**Figure 8**), and the intrusion of more mafic magma into a more evolved and/or stagnant magma system beneath a slow volcanic system (**Figure 9**). In both cases, as magma intrudes, I have attempted to show in a qualitative fashion how the different geochemical and geophysical indicators might vary as a group as a result of the intrusion process. In complex systems such as these, there are undoubtedly other processes which could modify or even reverse the changes shown here. Nevertheless, this is a first-order depiction of the changes which may be expected to occur from the introduction of new magmas beneath both types of volcanoes.

CONCLUDING REMARKS

The volume and ascent rate of new magma beneath a volcano is a first-order issue. In this regard, fast and slow volcanic systems present unique and different problems. At volcanoes with fast activity, the very short window available for forecasting is a significant impediment. From the limited data that are available, the window appears to be on the order of 1–3 months. However, the actual processes involved, such as intrusion and rise of magma to shallow crustal levels, can occur even faster, e.g., over several weeks in the case of Merapi, Mt. St. Helens, and Pinatubo, and possibly days to hours in the case of Chaitén. Hence identifying and using longer-term precursors at fast volcanic systems should be a future priority. At volcanoes with slow activity, the extended unrest can result in a situation where it is unclear (a) if magma is driving the unrest, and (b) if it is, whether the magma will reach the surface or not (see Moran et al., 2011). This uncertainty can persist for years and is well-illustrated by the events at Turrialba during the past several decades.

Mafic magma is clearly a significant component driving many if not all of these eruptions. In some cases its presence is obvious (e.g., Pinatubo, Soufrière Hills, Popocatépetl) and more cryptic elsewhere (e.g., Chaitén). Identifying the presence of mafic magma—as well as its volume, volatile content and buoyancy, and depth of interaction with resident magma—is a crucially important goal for understanding and forecasting fast and slow unrest. The longevity of slow systems may well

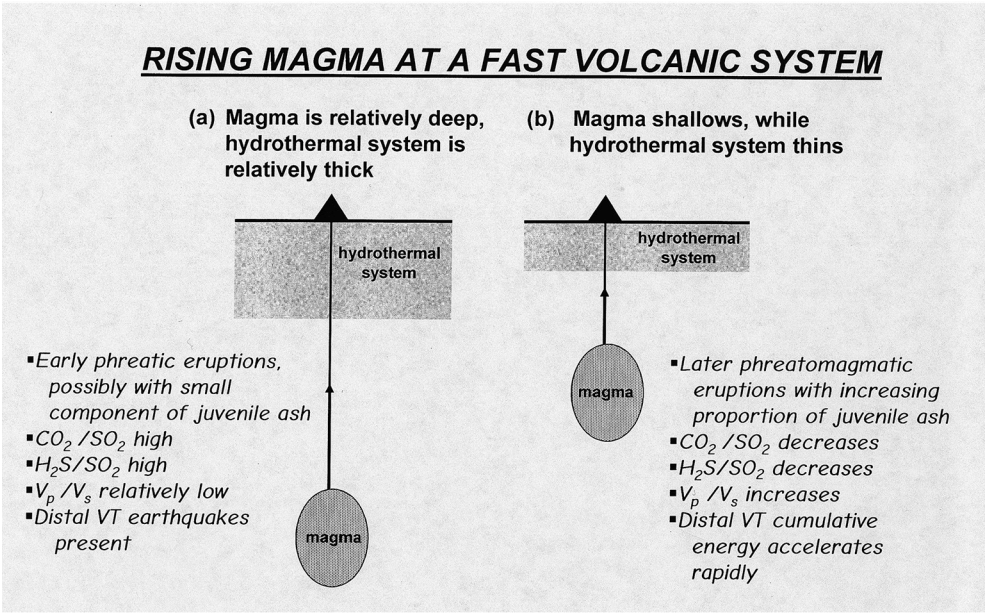

FIGURE 8 | A conceptual depiction of geochemical and geophysical change associated with rising magma at a volcano with fast activity. The hydrothermal system thins as the shallowing magma dries it.

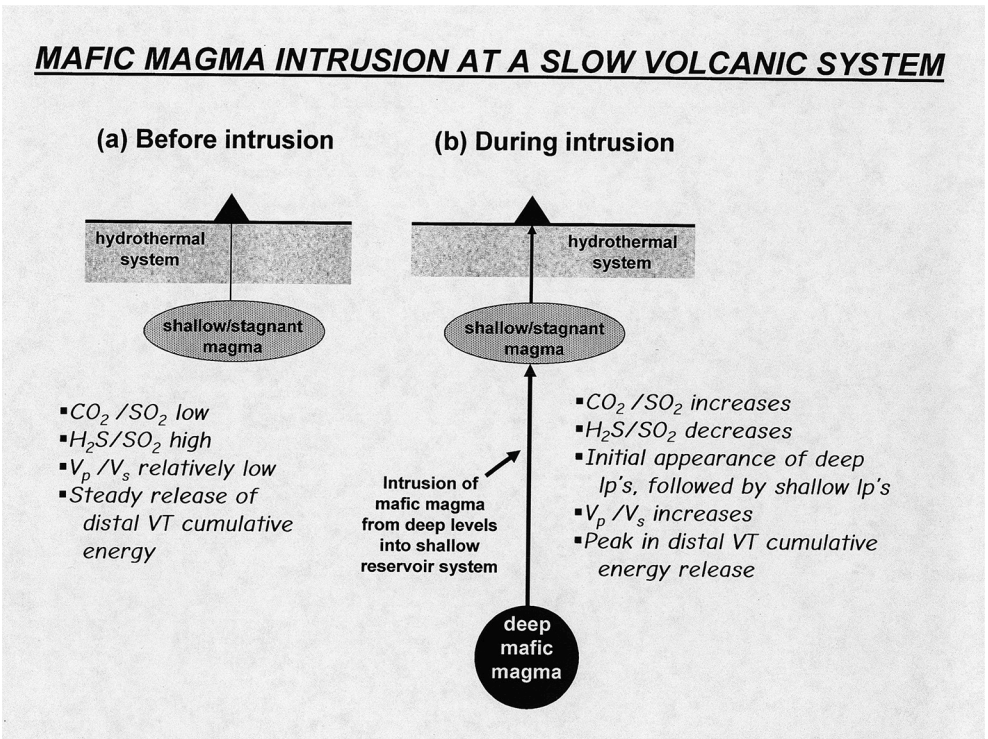

FIGURE 9 | A conceptual depiction of geochemical and geophysical change associated with intrusion of more mafic magma from deep levels at a volcano with slow activity.

depend upon repeated intrusions of new magma from deep levels into the shallow plumbing system. Understanding the timing of such intrusions is a major challenge. The forecasting approaches outlined above can help address and answer these questions.

It is possible that the distinction made in this paper between fast and slow behavior will ultimately prove too simplistic in terms of understanding and forecasting these systems. Refinements can and should be made where appropriate. Some systems could have extended periods of unrest terminated by paroxysmal activity. Other systems may produce a paroxysmal eruption initially, followed by lengthy unrest. Activity that is intermediate between fast and slow can also be envisaged. Many of the principles and ideas in this paper can be used to help comprehend such complex systems.

It is also possible that certain volcanoes are predisposed to fast behavior and others to slow behavior. Cosigüina volcano in Nicaragua appears to experience large explosive eruptions periodically during its history (Scott et al., 2006; Longpré et al., 2014), suggestive of repeated fast activity. In some cases, therefore, the plumbing system and crustal structure may be configured in such a way to promote fast or slow behavior. In other words, relatively large magma batches may be generated in the mantle at discrete times and transit rapidly through the crust beneath certain volcanoes (fast), while smaller magma batches move slowly through the crust under other volcanoes (slow).

At the earliest stages of unrest, it remains highly challenging to decide (a) if magma is involved, (b) the amount of magma, and (c) if subsequent activity will be fast, slow, or intermediate. Two key areas of future research include (1) precursory periods at volcanoes with fast behavior and (2) intrusion processes at volcanoes with slow behavior. Hopefully, this paper will provide some useful clues and suggestions to help answer these questions. Finally, it is worthwhile noting that the forecasting techniques discussed above do not necessarily entail large additional expenditures or infrastructure. Gas ratio measurements are inherently cheap, and they can be deployed effectively and rapidly on the ground and by drones. The advanced seismic analyses discussed above can be accomplished if a reasonably decent seismic network is in place. The magma volume calculation proposed by White and McCausland (2016) can be done with a single seismometer on a volcano. The exciting possibility is to see if these geochemical and geophysical techniques can be deployed and integrated effectively and rapidly in real time or near real time, in order to pinpoint a particular process or processes which may be occurring under or within a volcano.

AUTHOR CONTRIBUTIONS

The author confirms being the sole contributor of this work and approved it for publication.

FUNDING

The author acknowledges financial support from the Natural Sciences and Engineering Research Council of Canada through Discovery and Discovery Accelerator grants.

ACKNOWLEDGMENTS

The author acknowledges the extensive studies conducted by many researchers on the volcanoes discussed in this report. Conversations with Maarten de Moor and Stan Williams over a number of years have been very useful and insightful. The author thanks Rod Stewart of the Montserrat Volcano Observatory for permission to use the Soufrière Hills seismic data. The author acknowledges helpful comments by the Associate Editor Shan de Silva and the Editor Valerio Acocella, and reviews by Chris Newhall, Jan Lindsay, Greg Valentine, and two reviewers on earlier versions of this paper which helped to focus my ideas. The opinions and conclusions in this paper are not shared by all the reviewers, and the author is grateful to them for their viewpoints and insight. This work was supported by Discovery and Accelerator grants from the Natural Sciences and Engineering Research Council of Canada. All appropriate permissions have been obtained from the copyright holders of figures reproduced in the paper.

REFERENCES

Aiuppa, A., Federico, C., Giudice, G., and Gurrieri, S. (2005). Chemical mapping of a fumarolic field: La Fossa crater, Vulcano island (Aeolian Islands, Italy). *Geophys. Res. Lett.* 32:L13309. doi: 10.1029/2005GL023207

Aiuppa, A., Fischer, T. P., Plank, T., Robidoux, P., and Di Napoli, R. (2017). Along-arc, inter-arc and arc-to-arc variations in volcanic gas CO_2/S_T ratios reveal dual source of carbon in arc volcanism. *Earth Sci. Rev.* 168, 24–47. doi: 10.1016/j.earscirev.2017.03.005

Basualto, D., Peña, P., Delgado, C., Gallegos, C., Moreno, H., and Muñoz, J. O. (2008). Seismic activity related to the evolution of the explosive eruption of Chaitén volcano in the Southern Andes Volcanic Zone. *Eos Trans. AGU* 89:V43D2178B.

Blundy, J., Cashman, K. V., and Berlo, K. (2008). *Evolving Magma Storage Conditions Beneath Mount St. Helens Inferred from Chemical Variations in Melt Inclusions from the 1980-1986 and Current (2004-2006) Eruptions*. U.S. Geol. Surv. Prof. Pap. 1750, 755–790.

Budi-Santoso, A., Lesage, P., Dwiyono, S., Sumarti, S., Subandriyo, S., Jousset, P., et al. (2013). Analysis of the seismic activity associated with the 2010 eruption of Merapi volcano, Java. *J. Volcanol. Geotherm. Res.* 261, 153–170. doi: 10.1016/j.jvolgeores.2013.03.024

Campion, R., Martinez-Cruz, M., Lecocq, T., Caudron, C., Pacheco, J., Pinardi, G., et al. (2012). Space- and ground-based measurements of sulphur dioxide emissions from Turrialba volcano (Costa Rica). *Bull. Volcanol.* 74, 1757–1770. doi: 10.1007/s00445-012-0631-z

Carey, S., and Sigurdsson, H. (1985). The May 18, 1980 eruption of Mount St. Helens 2. Modeling of dynamics of the plinian phase. *J. Geophys. Res.* 90, 2948–2958.

Casadevall, T. J., Johnston, D. A., Harris, D. M., Rose, W. I. Jr., Malinconico, L. L., Stoiber, R. E., et al. (1981). *SO_2 Emission Rates at Mount St. Helens from March 29 Through December, 1980. The 1980 Eruptions of Mount St. Helens, Washington*, eds P. W. Lipman and D. R. Mullineaux. U.S. Geol. Surv. Prof. Pap. 1250, 193–200.

Cashman, K. V., and Hoblitt, R. P. (2004). Magmatic precursors to the 18 May 1980 eruption of Mount St. Helens, USA. *Geology* 32,141–144. doi: 10.1130/G20078.1

Castro, J. M., and Dingwell, D. B. (2009). Rapid ascent of rhyolitic magma at Chaitén volcano, Chile. *Nature* 461, 780–783. doi: 10.1038/nature08458

Christiansen, R. L., and Peterson, D. W. (1981). *Chronology of the 1980 Eruptive Activity. The 1980 Eruptions of Mount St. Helens, Washington*, eds P. W. Lipman and D. R. Mullineaux. U.S. Geol. Surv. Prof. Pap. 1250, 17–30.

Christopher, T. E., Blundy, J., Cashman, K., Cole, P., Edmonds, M., Smith, P. J., et al. (2015). Crustal-scale degassing due to magma system destabilization and magma-gas decoupling at Soufrière Hills volcano, Montserrat. *Geochem. Geophys. Geosyst.* 16, 2797–2811. doi: 10.1002/2015GC005791

Conde, V., Bredemeyer, S., Duarte, E., Pacheco, J. F., Miranda, S., Galle, B., et al. (2014). SO_2 degassing from Turrialba volcano linked to seismic signatures during the period 2008-2012. *Int. J. Earth Sci.* 103, 1983–1998. doi: 10.1007/s00531-013-0958-5

Daag, A. S., Tubianosa, B. S., Newhall, C. G., Tuñgol, N. M., Javier, D., Dolan, M. T., et al. (1996). "Monitoring sulphur dioxide emission at Mount Pinatubo," in *Fire and Mud: Eruptions and Lahars of Mount Pinatubo, Philippines*, eds C. G. Newhall and R. S. Punongbayan (Quezon; Seattle, WA: Philippine Institute of Volcanology and Seismology and University of Washington Press), 409–414.

De la Cruz-Reyna, S., Yokoyama, I., Martínez-Bringas, A., and Ramos, E. (2008). Precursory seismicity of the 1994 eruption of Popocatépetl volcano, central Mexico. *Bull. Volcanol.* 70, 753–767. doi: 10.1007/500445-008-0195-01

De Moor, J. M., Aiuppa, A., Avard, G., Wehrmann, H., Dunbar, N., Muller, C., et al. (2016). Turmoil at Turrialba volcano (Costa Rica): degassing and eruptive processes inferred from high-frequency gas monitoring. *J. Geophys. Res.* 121, 5761–5775. doi: 10.1002/2016JB013150

Delgado-Granados, H., Cárdenas González, L., and Piedad Sánchez, N. (2001). Sulfur dioxide emissions from Popocatépetl volcano (Mexico): case study of a high-emission rate, passively degassing erupting volcano. *J. Volcanol. Geotherm. Res.* 108, 107–120. doi: 10.1016/S0377-0273(00)00280-8

Doukas, M. P., and Gerlach, T. M. (1995). *Sulfur Dioxide Scrubbing During the 1992 Eruption of Crater Peak, Mount Spurr volcano, Alaska*. U.S. Geol. Surv. Bull. 2139, 47–57.

Drignon, M. J., Bechon, T., Arbaret, L., Burgisser, A., Komorowski, J.-C., Martel, C., et al. (2016). Preexplosive conduit conditions during the 2010 eruption of Merapi volcano (Java, Indonesia). *Geophys. Res. Lett.* 43, 11595–11602. doi: 10.1002/2016GL071153

Druitt, T. H., Young, S. R., Baptie, B., Bonadonna, C., Calder, E. S., Clarke, A. B., et al. (2002). Episodes of cyclic vulcanian explosive activity with fountain collapse at Soufrière Hills volcano, Montserrat. *Geol. Soc. Lond. Mem.* 21, 281–306. doi: 10.1144/GSL.MEM.2002.021.01.13

Endo, E. T., Malone, S. D., Noson, L. L., and Weaver, C. S. (1981). *Locations, Magnitudes, and Statistics of the March 20 – May 18 Earthquake Sequence. The 1980 Eruptions of Mount St. Helens, Washington*, eds P. W. Lipman and D. R. Mullineaux. U.S. Geol. Surv. Prof. Pap. 1250, 93–107.

Espíndola, J. M., Zamora-Camacho, A., and Jiménez, Z. (2006). Some aspects of the seismicity associated with the 1982 eruption of El Chichon volcano, Chiapas, Mexico. *J. Volcanol. Geotherm. Res.* 157, 367–374. doi: 10.1016/j.jvolgeores.2006.04.021

Ewert, J. W., Lockhart, A. B., Marcial, S., and Ambubuyog, G. (1996). "Ground deformation prior to the 1991 eruptions of Mount Pinatubo," in *Fire and Mud: Eruptions and Lahars of Mount Pinatubo, Philippines*, eds C. G. Newhall and R. S. Punongbayan (Quezon; Seattle, WA: Philippine Institute of Volcanology and Seismology and University of Washington Press), 329–338.

GVN Bulletin (1996). Turrialba. *GVN Bull.* 21, 7.

Gómez-Vazquez, A., De la Cruz-Reyna, S., and Mendoza-Rosas, A. T. (2016). The ongoing dome emplacement and destruction cyclic process at Popocatépetl volcano, central Mexico. *Bull. Volcanol.* 78, 2–15. doi: 10.1007/s00445-016-1054-z,

Hall, M. L. (1990). Chronology of the principal scientific and governmental actions leading up to the November 13, 1985 eruption of Nevado del Ruiz, Colombia. *J. Volcanol. Geotherm. Res.* 42, 101–115.

Harlow, D. H., Power, J. A., Laguerta, E. P., Ambubuyog, G., White, R. A., and Hoblitt, R. P. (1996). "Precursory seismicity and forecasting of the June 15, 1991, eruption of Mount Pinatubo," in *Fire and Mud: Eruptions and Lahars of Mount Pinatubo, Philippines*, eds C. G. Newhall and R. S. Punongbayan (Quezon; Seattle, WA: Philippine Institute of Volcanology and Seismology and University of Washington Press), 285–305.

Hobbs, P. V., Radke, L. F., Eltgroth, M. W., and Hegg, D. A. (1981). Airborne studies of the emissions from the volcanic eruptions of Mount St. Helens. *Science* 211, 816–818.

Hofstetter, A., and Malone, S. D. (1986). Observations of volcanic tremor at Mount St. Helens in April and May 1980. *Bull. Seismol. Soc. Am.* 76, 923–938.

Huang, H.-H., Lin, F.-C., Schmandt, B., Farrell, J., Smith, R. B., and Tsai, V. C. (2015). The Yellowstone magmatic system from the mantle plume to the upper crust. *Science* 348, 773–776. doi: 10.1126/science.aaa5648

Husen, S., Smith, R. B., and Waite, G. P. (2004). Evidence for gas and magmatic sources beneath the Yellowstone volcanic field from seismic tomographic imaging. *J. Volcanol. Geotherm. Res.* 131, 397–410. doi: 10.1016/S0377-0273(03)00416-5

Jiménez, Z., Espíndola, V. H., and Espíndola, J. M. (1999). Evolution of the seismic activity from the 1982 eruption of El Chichon volcano, Chiapas, Mexico. *Bull. Volcanol.* 61, 411–422.

Jousset, P., Budi-Santoso, A., Jolly, A. D., Boichu, M., Surono, Dwiyono, S., et al. (2013). Signs of magma ascent in LP and VLP seismic events and link to degassing: an example from the 2010 explosive eruption at Merapi volcano, Indonesia. *J. Volcanol. Geotherm. Res.* 261, 171–192. doi: 10.1016/j.jvolgeores.2013.03.014

Kokelaar, B. P. (2002). Setting, chronology and consequences of the eruption of Soufrière Hills volcano, Montserrat (1995-1999). *Geol. Soc. Lond. Mem.* 21, 1–43. doi: 10.1144/GSL.MEM.2002.021.01.02

Komorowski, J.-C., Jenkins, S., Baxter, P. J., Picquout, A., Lavigne, F., Charbonnier, S., et al. (2013). Paroxysmal dome explosion during the Merapi 2010 eruption: processes and facies relationships of associated high-energy pyroclastic density currents. *J. Volcanol. Geotherm. Res.* 261, 260–294. doi: 10.1016/j.jvolgeores.2013.01.007

Koulakov, I., West, M., and Izbekov, P. (2013). Fluid ascent during the 2004-2005 unrest at Mt. Spurr inferred from seismic tomography. *Geophys. Res. Lett.* 40, 4579–4582. doi: 10.1002/grl.50674

Kumagai, H., Maeda, Y., Londoño, J., López, C., Castaño, L., Galvis, B., et al. (2017). *Magma Conduit System Beneath Nevado del Ruiz volcano, Colombia, Inferred from Seismic Waveform Analysis*. Portland, OR: IAVCEI General Assembly.

Lange, D., Rietbrock, A., Haberland, C., Bataille, K., Dahm, T., Tilmann, F., et al. (2007). Seismicity and geometry of the south Chilean subduction zone (41.5°S—43.5°S): implications for controlling parameters. *Geophys. Res. Lett.* 34, L06311. doi: 10.1029/2006GL029190

Lara, L. E., Moreno, R., Amigo, Á., Hoblitt, R. P., and Pierson, T. C. (2013). Late Holocene history of Chaitén volcano: new evidence for a 17th century eruption. *Andean Geol.* 40, 249–261. doi: 10.5027/andgeoV40n2-a04

Lipman, P. W., Moore, J. G., and Swanson, D. A. (1981). *Bulging of the North Flank before the May 18 Eruption – Geodetic Data. The 1980 Eruptions of Mount St. Helens, Washington*, eds P. W. Lipman and D. R. Mullineaux. U.S. Geol. Surv. Prof. Pap. 1250, 143–155.

Londoño, J. M. (2016). Evidence of recent deep magmatic activity at Cerro Bravo-Cerro Machín volcanic complex, central Colombia. Implications for future volcanic activity at Nevado del Ruiz, Cerro Machín and other volcanoes. *J. Volcanol. Geotherm. Res.* 324, 156–168. doi: 10.1016/j.jvolgeores.2016.06.003

Londoño, J. M., and Kumagai, H. (2018). 4D seismic tomography of Nevado del Ruiz volcano, Colombia, 2000-2016. *J. Volcanol. Geotherm. Res.* doi: 10.1016/j.jvolgeores.2018.02.015

Longpré, M.-A., Stix, J., Costa, F., Espinoza, E., and Muñoz, A. (2014). Magmatic processes and associated timescales leading to the January 1835 eruption of Cosigüina volcano, Nicaragua. *J. Petrol.* 55, 1173–1201. doi: 10.1093/petrology/egu022. [Epub ahead of print].

Lundgren, P., Samsonov, S. V., López Velez, C. M., and Ordoñez, M. (2015). Deep source model for Nevado del Ruiz volcano, Colombia, constrained by interferometric synthetic aperture radar observations. *Geophys. Res. Lett.* 42, 4816–4823. doi: 10.1002/2015GL063858

Macías, J. L., and Siebe, C. (2005). Popocatépetl's crater filled to the brim: significance for hazard evaluation. *J. Volcanol. Geotherm. Res.* 141, 327–330. doi: 10.1016/j.jvolgeores.2004.10.005

Major, J. J., and Lara, L. E. (2013). Overview of Chaitén volcano, Chile, and its 2008-2009 eruption. *Andean Geol.* 40, 196–215. doi: 10.5027/andgeoV40n2-a01

Mann, C. P., Wallace, P. J., and Stix, J. (2013). Phenocryst-hosted melt inclusions record stalling of magma during ascent in the conduit and upper magma reservoir prior to vulcanian explosions, Soufrière Hills volcano, Montserrat, West Indies. *Bull. Volcanol.* 75, 687. doi: 10.1007/s00445-013-0687-4

Martinelli, B. (1990). Analysis of seismic patterns observed at Nevado del Ruiz volcano, Colombia during August – September 1985. *J. Volcanol. Geotherm. Res.* 41, 297–314.

Martini, F., Tassi, F., Vaselli, O., Del Potro, R., Martinez, M., Van del Laat, R., et al. (2010). Geophysical, geochemical and geodetic signals of reawakening at Turrialba volcano (Costa Rica) after almost 150 years of quiescence. *J. Volcanol. Geotherm. Res.* 198, 416–432. doi: 10.1016/j.jvolgeores.2010.09.021

Moore, J. G., and Albee, W. C. (1981). *Topographic and Structural Changes, March-July 1980 – Photogrammetric Data. The 1980 Eruptions of Mount St. Helens, Washington*, eds P. W. Lipman and D. R. Mullineaux. U.S. Geol. Surv. Prof. Pap. 1250, 123–134.

Moran, S. C., Newhall, C., and Roman, D. C. (2011). Failed magmatic eruptions: late-stage cessation of magma ascent. *Bull. Volcanol.* 73, 115–122. doi: 10.1007/ss00445-010-0444-x

Naranjo, J. A., and Stern, C. R. (2004). Holocene tephrochronology of the southernmost part (42°30′-45°S) of the Andean Southern Volcanic Zone. *Rev. Geol. Chile* 31, 225–240. doi: 10.4067/S0716-02082004000200003

Naranjo, J. L., Sigurdsson, H., Carey, S. N., and Fritz, W. (1986). Eruption of the Nevado del Ruiz volcano, Colombia, on 13 November 1985: tephra fall and lahars. *Science* 233, 961–963.

Newhall, C. G., Daag, A. S., Delfin, F. G. Jr., Hoblitt, R. P., McGeehin, J., Pallister, J. S., et al. (1996). "Eruptive history of Mount Pinatubo," in *Fire and Mud: Eruptions and Lahars of Mount Pinatubo, Philippines*, eds C. G. Newhall and R. S. Punongbayan (Quezon; Seattle, WA: Philippine Institute of Volcanology and Seismology and University of Washington Press), 165–195.

Pallister, J. S., Diefenbach, A. K., Burton, W. C., Muñoz, J., Griswold, J. P., Lara, L. E., et al. (2013). The Chaitén rhyolite lava dome: eruption sequence, lava dome volumes, rapid effusion rates and source of the rhyolite magma. *Andean Geol.* 40, 277–294. doi: 10.5027/andgeoV40n2-a06

Pallister, J. S., Hoblitt, R. P., Crandell, D. R., and Mullineaux, D. R. (1992). Mount St. Helens a decade after the 1980 eruptions: magmatic models, chemical cycles, and a revised hazards assessment. *Bull. Volcanol.* 54, 126–146.

Pallister, J. S., Hoblitt, R. P., Meeker, G. P., Knight, R. J., and Siems, D. F. (1996). "Magma mixing at Mount Pinatubo: petrographic and chemical evidence from the 1991 deposits," in F*ire and Mud: Eruptions and Lahars of Mount Pinatubo, Philippines*, eds C. G. Newhall and R. S. Punongbayan (Quezon; Seattle, WA: Philippine Institute of Volcanology and Seismology and University of Washington Press), 687–731.

Pardo, N., Cronin, S. J., Németh, K., Brenna, M., Schipper, C. I., Breard, E., et al. (2014). Perils in distinguishing phreatic from phreatomagmatic ash; insights into the eruption mechanisms of the 6 August 2012 Mt. Tongariro eruption, New Zealand. *J. Volcanol. Geotherm. Res.* 286, 397–414. doi: 10.1016/j.jvolgeores.2014.05.001

Patanè, D., Barberi, G., Cocina, O., De Gori, P., and Chiarabba, C. (2006). Time-resolved seismic tomography detects magma intrusions at Mount Etna. *Science* 313, 821–823. doi: 10.1126/science.1127724

Preece, K., Gertisser, R., Barclay, J., Berlo, K., Herd, R. A., and Edinburgh Ion Microprobe Facility (2014). Pre- and syn-eruptive degassing and crystallisation processes of the 2010 and 2006 eruptions of Merapi volcano, Indonesia. *Contrib. Miner. Petrol.* 168, 1061. doi: 10.1007/s00410-014-1061-z

Robertson, R., Cole, P., Sparks, R. S. J., Harford, C., Lejeune, A. M., McGuire, W. J., et al. (1998). The explosive eruption of Soufrière Hills volcano, Montserrat, West Indies, 17 September, 1996. *Geophys. Res. Lett.* 25, 3429–3432.

Rutherford, M. J., and Devine, J. D. (1996). "Preeruption pressure-temperature conditions and volatiles in the 1991 dacitic magma of Mount Pinatubo," in *Fire and Mud: Eruptions and Lahars of Mount Pinatubo, Philippines*, eds C. G. Newhall and R. S. Punongbayan (Quezon; Seattle, WA: Philippine Institute of Volcanology and Seismology and University of Washington Press), 751–766.

Rutherford, M. J., Sigurdsson, H., Carey, S., and Davis, A. (1985). The May 18, 1980, eruption of Mount St. Helens 1. Melt composition and experimental phase equilibria. *J. Geophys. Res.* 90, 2929–2947.

Sabit, J. P., Pigtain, R. C., and de la Cruz, E. G. (1996). "The west-side story: observations of the 1991 Mount Pinatubo eruptions from the west," in *Fire and Mud: Eruptions and Lahars of Mount Pinatubo, Philippines*, eds C. G. Newhall and R. S. Punongbayan (Quezon; Seattle, WA: Philippine Institute of Volcanology and Seismology and University of Washington Press), 445–455.

Sandri, L., Acocella, V., and Newhall, C. (2017). Searching for patterns in caldera unrest. *Geochem. Geophys. Geosyst.* 18, 2748–2768. doi: 10.1002/2017GC006870

Sarna-Wojcicki, A. M., Waitt, R. B. Jr., Woodward, M. J., Shipley, S., and Rivera, J. (1981). *Premagmatic Ash Erupted from March 27 Through May 14, 1980 – Extent, Mass, Volume, and Composition. The 1980 Eruptions of Mount St. Helens, Washington*, eds P. W. Lipman and D. R. Mullineaux. U.S. Geol. Surv. Prof. Pap. 1250, 569–575.

Scott, W. E., Hoblitt, R. P., Torres, R. C., Self, S., Martinez, M. M. L., and Nillos, T. Jr. (1996). "Pyroclastic flows of the June 15, 1991, climactic eruption of Mount Pinatubo," in *Fire and Mud: Eruptions and Lahars of Mount Pinatubo, Philippines*, eds C. G. Newhall and R. S. Punongbayan (Quezon; Seattle, WA: Philippine Institute of Volcanology and Seismology and University of Washington Press), 545–570.

Scott, W., Gardner, C., Devoli, G., and Alvarez, A. (2006). The A.D. 1835 eruption of Volcán Cosigüina, Nicaragua: A guide for assessing local volcanic hazards. *Geol. Soc. Am. Spec. Pap.* 412, 167-187. doi: 10.1130/2006.2412(09)

Shinohara, H. (2005). A new technique to estimate volcanic gas composition: plume measurements with a portable multi-sensor system. *J. Volcanol. Geotherm. Res.* 143, 319–333. doi: 10.1016/j.jvolgeores.2004.12.004

Sparks, R. S. J., and Cashman, K. V. (2017). Dynamic magma systems: implications for forecasting volcanic activity. *Elements* 13, 35–40. doi: 10.2113/gselements.13.1.35

Sparks, R. S. J., and Young, S. R. (2002). The eruption of Soufrière Hills volcano, Montserrat (1995-1999): overview of scientific results. *Geol. Soc. Lond. Mem.* 21, 45–69. doi: 10.1144/GSL.MEM.2002.021.01.03

Stix, J., and de Moor, M. (2018). Understanding and forecasting phreatic eruptions driven by magmatic degassing. *Earth Planets Space*. 70:83. doi: 10.1186/S40623-018-0855-z

Stix, J., Layne, G. D., and Williams, S. N. (2003). Mechanisms of degassing at Nevado del Ruiz volcano, Colombia. *J. Geol. Soc. London* 160, 507–521.

Surono, Jousset, P., Pallister, J., Boichu, M., Buongiorno, M. F., Budisantoso, A., et al. (2012). The 2010 explosive eruption of Java's Merapi volcano – a '100-year' event. *J. Volcanol. Geotherm. Res.* 241–242, 121–135. doi: 10.1016/j.jvolgeores.2012.06.018

Symonds, R. B., and Gerlach, T. M. (1998). "Modeling the interaction of magmatic gases with water at active volcanoes," in *Water-Rock Interaction: Proceedings of the 9th International Symposium of Water-Rock Interaction*, eds G. B. Arehart and J. R. Hulston (Rotterdam: Balkema), 495–498.

Vargas, C. A., Koulakov, I., Jaupart, C., Gladkov, V., Gomez, E., El Khrepy, S., et al. (2017). Breathing of the Nevado del Ruiz volcano reservoir, Colombia, inferred from repeated seismic tomography. *Sci. Rep.* 7:46094. doi: 10.1038/srep46094

Voight, B., Hoblitt, R. P., Clarke, A. B., Lockhart, A. B., Miller, A. D., Lynch, L., et al. (1998). Remarkable cyclic ground deformation monitored in real-time on Montserrat, and its use in eruption forecasting. *Geophys. Res. Lett.* 25, 3405–3408.

Wadge, G., and Isaacs, M. C. (1988). Mapping the volcanic hazards from the Soufriere Hills volcano, Montserrat, West Indies using an image processor. *J. Geol. Soc. Lond.* 145, 541–551.

Westrich, H. R., and Gerlach, T. M. (1992). Magmatic gas source for the stratospheric SO_2 cloud from the June 15,1991, eruption of Mount Pinatubo. *Geology* 20, 867–870.

White, R. A. (1996). "Precursory deep long-period earthquakes at Mount Pinatubo: spatio-temporal link to a basalt trigger," in *Fire and Mud: Eruptions and Lahars of Mount Pinatubo, Philippines*, eds C. G. Newhall and R. S. Punongbayan (Quezon; Seattle, WA: Philippine Institute of Volcanology and Seismology and University of Washington Press), 307–327.

White, R., and McCausland, W. (2016). Volcano-tectonic earthquakes: a new model for estimating intrusive volumes and forecasting eruptions. *J. Volcanol. Geotherm. Res.* 309, 139–155. doi: 10.1016/j.jvolgeores.2015.10.020

Wicks, C., de la Llera, J. C., Lara, L. E., and Lowenstern, J. (2011). The role of dyking and fault control in the rapid onset of eruption at Chaitén volcano, Chile. *Nature* 478, 374–377. doi: 10.1038/nature10541

Wiebe, R. A. (1994). Silicic magma chambers as traps for basaltic magmas: the Cadillac Mountain intrusive complex, Mount Desert Island, Maine. *J. Geol.* 102, 423–437.

Witter, J. B., Kress, V. C., and Newhall, C. G. (2005). Volcán Popocatépetl, Mexico. Petrology, magma mixing, and intermediate sources of volatiles for the 1994 - present eruption. *J. Petrol.* 46, 2337–2366. doi: 10.1093/petrology/egi058

Wolfe, E. W., and Hoblitt, R. P. (1996). "Overview of the eruptions," in *Fire and Mud: Eruptions and Lahars of Mount Pinatubo, Philippines*, eds C. G. Newhall and R. S. Punongbayan (Quezon; Seattle, WA: Philippine Institute of Volcanology and Seismology and University of Washington Press), 3–20.

Conflict of Interest Statement: The author declares that the research was conducted in the absence of any commercial or financial relationships that could be construed as a potential conflict of interest.